Superfluid transition temperature and fluctuation theory of spin-orbit- and Rabi-coupled fermions with tunable interactions

Philip D. Powell,[1,2] Gordon Baym,[2] and C. A. R. Sá de Melo[3]

[1]*Lawrence Livermore National Laboratory, 7000 East Avenue, Livermore, California 94550, USA*

[2]*Department of Physics, University of Illinois at Urbana-Champaign, 1110 W. Green Street, Urbana, Illinois 61801, USA*

[3]*School of Physics, Georgia Institute of Technology, 837 State Street, Atlanta, Georgia 30332, USA*

(Received 27 January 2022; accepted 23 May 2022; published 6 June 2022)

We obtain the superfluid transition temperature of equal Rashba-Dresselhaus spin-orbit- and Rabi-coupled Fermi superfluids, from the Bardeen-Cooper-Schrieffer (BCS) to Bose-Einstein condensate (BEC) regimes in three dimensions for tunable s-wave interactions. In the presence of Rabi coupling, we find that spin-orbit coupling enhances (reduces) the critical temperature in the BEC (BCS) limit. For fixed interactions, we show that spin-orbit coupling can convert a first-order (discontinuous) phase transition into a second-order (continuous) phase transition, as a function of Rabi coupling. We derive the Ginzburg-Landau free energy to sixth power in the superfluid order parameter to describe both continuous and discontinuous phase transitions as a function of spin-orbit and Rabi couplings. Lastly, we develop a time-dependent Ginzburg-Landau fluctuation theory for an arbitrary mixture of Rashba and Dresselhaus spin-orbit couplings at any interaction strength.

DOI: 10.1103/PhysRevA.105.063304

I. INTRODUCTION

The ability to simulate magnetic and other external fields [1–12] in cold atomic gases has created the opportunity to explore a wide variety of new interactions and complex phase structures otherwise inaccessible in the laboratory. Moreover, the capacity to generate these synthetic fields in both bosonic and fermionic systems, and to continuously tune two-body interactions by means of a Feshbach resonance, has opened up a wonderland of tunable systems, previously restricted to theorists' dreams. For example, the possibility of simulating quantum chromodynamics (QCD) on an optical lattice [13–16] is a tantalizing prospect for researchers whose current theoretical tools remain limited by QCD's nonperturbative character and the restriction of lattice techniques to near-zero chemical potential.

Previous theoretical analyses of three-dimensional spin-orbit-coupled Fermi gases (e.g., ^{6}Li, ^{40}K) have focused mainly on the zero-temperature limit, in which several exotic phases characterized by unconventional pairing are expected to emerge [17–22]. However, the Raman laser platforms currently employed to produce synthetic spin-orbit fields also induce heating that prevents the realization of temperatures sufficiently low to observe the superfluid transition in either the weakly coupled Bardeen-Cooper-Schrieffer (BCS) or the strongly coupled Bose-Einstein condensate (BEC) regimes [5,7]. Thus, while two-body bound states (Feshbach molecules) have been observed in the BEC limit of ^{40}K [7,23], the observation of superfluid states remain elusive. Future experiments, however, may break this impasse by employing a new platform currently under development—the radio frequency atom chip—which avoids heating of the atom cloud entirely [24]. While rf atom chips are somewhat more restricted than the Raman scheme in the maximum obtainable spin-orbit coupling, its potential to reach superfluid temperatures is leading to its adoption in the next generation of experiments probing the topological superfluid phases of spin-orbit-coupled fermions [25].

One class of systems of particular interest in the context of quantum simulation is that of Rashba-Dresselhaus spin-orbit-coupled gases [17–22,26,27]. These systems are intriguing both because they reflect physics studied extensively in the context of semiconductors [28,29] and because they provide a platform for realizing tunable non-Abelian fields in the laboratory. Thus, while the holy grail of a full optical simulation of QCD remains years in the future, there do exist notable analogies between quark matter and cold atomic systems (e.g., non-Abelian fields, evolution between strongly and weakly coupled limits) within near-term experimental reach [30–33]. Investigations of spin-orbit-coupled ultracold gases have also included optical lattices [34–43], thus enlarging the number of possible physical systems that can be accessible experimentally.

To date, most experimental realizations of these systems have adopted equal Rashba-Dresselhaus couplings [4–6,44], but systems exhibiting Rashba-only couplings have also been created [11,45,46]. Other experiments have generated spin-orbit coupling dynamically [47] or even created three-dimensional spin-orbit coupling [48]. Due to the versatility of Rashba-Dresselhaus coupled systems, the ability to realize these systems in the laboratory, and the myriad technical challenges inherent in reaching arbitrarily low temperatures, it is increasingly important to provide a theoretical framework for guiding and testing these simulators against experimental probes at realistic (nonzero) temperatures.

This problem bears a close relation to spin-orbit coupling in solids, where the role of the Rabi frequency is played by an external Zeeman magnetic field. While a mean-field treatment

describes well the evolution from the BCS to the BEC regime at zero temperature [49,50], this order of approximation fails to describe the correct critical temperature of the system in the BEC regime because the physics of two-body bound states, i.e., Feshbach molecules, is not captured when the pairing order parameter goes to zero [51]. To remedy this problem, we include the effects of order-parameter fluctuations in the thermodynamic potential.

In this paper, we investigate the impact of a specific class of spin-orbit coupling, namely, an equal mixture of Rasha and Dresselhaus terms, on the superfluid transition temperature of a three-dimensional Rabi-coupled Fermi gas, but also give general results for an arbitrary mixture of Rashba and Dresselhaus components. This paper is the longer version of our preliminary work [52]. We stress that the present results are applicable to both neutral cold atomic and charged condensed-matter systems. We show that spin-orbit coupling, in the presence of a Rabi field (or Zeeman field, in solids), enhances the critical temperature of the superfluid in the BEC regime and converts a discontinuous first-order phase transition into a continuous second-order transition, as a function of the Rabi frequency for given two-body interactions. We analyze the nature of the phase transition in terms of the Ginzburg-Landau free energy, calculating it to the sixth power of the superfluid order parameter, as required to describe both discontinuous transitions as a function of the spin-orbit coupling, Rabi frequency, and two-body interactions.

This paper is organized as follows. In Sec. II, we describe the Hamiltonian and action for three-dimensional Fermi gases in the presence of a general Rashba-Dresselhaus spin-orbit coupling, Rabi field, and tunable s-wave interactions. We also obtain the inverse Green operator that is used in the calculation of the thermodynamic potential and Ginzburg-Landau theory of subsequent sections. In Sec. III, we analyze the thermodynamic potential across the entire BCS-to-BEC evolution, including contributions from both the mean-field and Gaussian fluctuations, and obtain the order-parameter and number equations. In Sec. IV, we study the combined effects of Rabi fields and spin-orbit coupling on the superfluid critical temperature, constructing the finite-temperature phase diagram versus Rabi fields and scattering parameter. In Sec. V, we present the Ginzburg-Landau (GL) theory for the superfluid order parameter and investigate further corrections to the critical temperature in the BEC limit by including interactions between bosonic bound states. The GL action is obtained to sixth order in the order parameter to allow for the existence of discontinuous (first-order) phase transitions. In Sec. VI, we compare our work on the experimentally relevant equal Rashba-Dresselhaus spin-orbit coupling with earlier work that has considered different forms of theoretically motivated spin-orbit couplings. In Sec. VII, we conclude and look toward the future of experimental work in this field.

In the interest of readability, we relegate a number of detailed calculations to Appendices. In Appendix A, we discuss the Hamiltonian and effective Lagrangian for a general Rashba-Dresselhaus spin-orbit coupling. In Appendix B, we analyze the saddle-point approximation for general Rashba-Dresselhaus spin-orbit coupling. In Appendix C, we derive the modified number equation, including the contribution arising from Gaussian fluctuations, which renormalizes the chemical potential obtained at the saddle-point level. In Appendix D, using a general Rashba-Dresselhaus spin-orbit coupling, we obtain expressions for the coefficients of the Ginzburg-Landau theory up to sixth order in order parameter.

II. HAMILTONIAN AND ACTION

Throughout this paper, we adopt units in which $\hbar = k_B = 1$. The Hamiltonian density of a three-dimensional Fermi gas in the presence of Rashba-Dresselhaus spin-orbit coupling and Rabi field is

$$\mathcal{H}(\mathbf{r}) = \mathcal{H}_k(\mathbf{r}) + \mathcal{H}_{so}(\mathbf{r}) + \mathcal{H}_I(\mathbf{r}) - \mu n(\mathbf{r}). \tag{1}$$

The first term in Eq. (1) is the kinetic energy,

$$\mathcal{H}_k(\mathbf{r}) = \sum_s \psi_s^\dagger(\mathbf{r}) \frac{\hat{\mathbf{k}}^2}{2m} \psi_s(\mathbf{r}), \tag{2}$$

where $\hat{\mathbf{k}} = -i\boldsymbol{\nabla}$ is the momentum operator, $\psi_s(\mathbf{r})$ is the fermion field at position $\mathbf{r}$ with (real or pseudo-) spin s and mass m. The second term is the spin-orbit interaction,

$$\mathcal{H}_{so}(\mathbf{r}) = \sum_{ss'} \psi_s^\dagger(\mathbf{r}) [\mathbf{H}_{\rm so}(\hat{\mathbf{k}})]_{ss'} \psi_{s'}(\mathbf{r}), \tag{3}$$

with the spin-orbit-coupling matrix in momentum ($\mathbf{k}$) space being

$$\mathbf{H}_{\rm so}(\hat{\mathbf{k}}) = \frac{\kappa}{m}(\hat{k}_x \boldsymbol{\sigma}_x + \eta \hat{k}_y \boldsymbol{\sigma}_y) - \frac{\Omega_R}{2}\boldsymbol{\sigma}_z, \tag{4}$$

where $(\boldsymbol{\sigma}_x, \boldsymbol{\sigma}_y, \boldsymbol{\sigma}_z)$ are the Pauli matrices in spin space, κ is the momentum transfer to the atoms in a two-photon Raman process [7] or on a radio frequency atom chip [24], η is the anisotropy of the Rashba-Dresselhaus field, and Ω_R is the Rabi frequency. The third term is the two-body s-wave contact interaction,

$$\mathcal{H}_I(\mathbf{r}) = -g\psi_\uparrow^\dagger(\mathbf{r})\psi_\downarrow^\dagger(\mathbf{r})\psi_\downarrow(\mathbf{r})\psi_\uparrow(\mathbf{r}), \tag{5}$$

where $g > 0$ corresponds to a constant attraction between opposite spins. Finally, μ is the chemical potential and $n(\mathbf{r}) = \sum_s \psi_s^\dagger(\mathbf{r})\psi_s(\mathbf{r})$ is the local density. While the general Rashba-Dresselhaus spin-orbit coupling is discussed in Appendix A, in what follows we focus on the more experimentally relevant situation of equal Rashba and Dresselhaus couplings ($\eta = 0$).

Standard manipulations (see Appendix A) lead to the Lagrangian density,

$$\mathcal{L}(\mathbf{r},\tau) = \frac{1}{2}\Psi^\dagger(\mathbf{r},\tau)\mathbf{G}^{-1}(\hat{\mathbf{k}},\tau)\Psi(\mathbf{r},\tau) + \frac{1}{g}|\Delta(\mathbf{r},\tau)|^2 + K(\hat{\mathbf{k}})\delta(\mathbf{r}-\mathbf{r}'), \tag{6}$$

where $\tau = it$ is the imaginary time, $\Psi = (\psi_\uparrow \psi_\downarrow \psi_\uparrow^\dagger \psi_\downarrow^\dagger)^T$ is the Nambu spinor, $K(\hat{\mathbf{k}}) = \hat{\mathbf{k}}^2/2m - \mu$ is the kinetic energy operator with respect to the chemical potential, and $\Delta(\mathbf{r},\tau) = -g\langle\psi_\downarrow(\mathbf{r},\tau)\psi_\uparrow(\mathbf{r},\tau)\rangle$ is the pairing field describing the formation of pairs of two fermions with opposite spins. Note that μ includes the overall positive shift $\kappa^2/2m$ in the single-particle kinetic energies due to spin-orbit coupling. The

inverse Green's operator appearing in Eq. (6) is

$$\mathbf{G}^{-1}(\hat{\mathbf{k}},\tau)=\begin{pmatrix}\partial_\tau-K_\uparrow & -i\kappa\hat{k}_x/m & 0 & -\Delta\\ i\kappa\hat{k}_x/m & \partial_\tau-K_\downarrow & \Delta & 0\\ 0 & \Delta^* & \partial_\tau+K_\uparrow & -i\kappa\hat{k}_x/m\\ -\Delta^* & 0 & i\kappa\hat{k}_x/m & \partial_\tau+K_\downarrow\end{pmatrix}, \tag{7}$$

where $K_{\uparrow,\downarrow}=K(\hat{\mathbf{k}})\mp\Omega_R/2$, are the kinetic energy terms shifted by the Rabi coupling.

As noted above, a mean-field treatment of this Lagrangian fails to correctly describe the superfluid critical temperature in the BEC regime. However, the inclusion of Gaussian fluctuations of Δ captures the effects of two-body bound states and leads to a physical superfluid transition temperature. It is to this task that we now turn.

III. THERMODYNAMIC POTENTIAL

The system's partition function may be expressed in terms of the functional integral,

$$\mathcal{Z}=\int\mathcal{D}\Delta\mathcal{D}\Delta^*\mathcal{D}\Psi\mathcal{D}\Psi^\dagger e^{-\mathcal{S}}, \tag{8}$$

where the Euclidean action is

$$\mathcal{S}=\int_0^\beta d\tau\int d^3\mathbf{r}\mathcal{L}(\mathbf{r},\tau), \tag{9}$$

$\beta=1/T$ is the inverse temperature, and the Lagrangian density is given by Eq. (6). Integrating over the fermion fields yields the thermodynamic potential,

$$\Omega=-T\ln\mathcal{Z}=\Omega_0+\Omega_F, \tag{10}$$

where $\Omega_0=-T\ln\mathcal{Z}_0=TS_0$ is the mean-field (saddle-point) contribution, for which $\Delta(\mathbf{r},\tau)=\Delta_0$, and $\Omega_F=-T\ln\mathcal{Z}_F$ is the contribution arising from order-parameter fluctuations. Detailed derivations of the thermodynamic potential for a general Rashba-Dresselhaus spin-orbit coupling, as well as the associated order-parameter and number equations, are given in Appendices B and C. The contributions to the thermodynamic potential for the experimentally relevant situation of equal Rashba-Dresselhaus spin-orbit coupling are discussed below in Sec. III A at the mean-field and in Sec. III B at the Gaussian fluctuation level.

A. Mean-field approximation

The mean-field, or saddle-point, term in the thermodynamic potential is

$$\Omega_0=V\frac{|\Delta_0|^2}{g}-\frac{T}{2}\sum_{\mathbf{k},j}\ln[1+e^{-\beta E_j(\mathbf{k})}]+\sum_{\mathbf{k}}\xi_{\mathbf{k}}, \tag{11}$$

where $\xi_{\mathbf{k}}=\varepsilon_{\mathbf{k}}-\mu$, $\varepsilon_{\mathbf{k}}=\mathbf{k}^2/2m$, and the $E_j(\mathbf{k})$, with $j=\{1,2,3,4\}$, are the eigenvalues of the momentum space Nambu Hamiltonian matrix,

$$\mathbf{H}_0(\mathbf{k})=\boldsymbol{\partial}_\tau-\mathbf{G}^{-1}(\mathbf{k},\tau)|_{\Delta=\Delta_0}, \tag{12}$$

where the operator $\boldsymbol{\partial}_\tau=\mathbf{I}\partial_\tau$, and $\mathbf{I}$ is the identity matrix. The first set of eigenvalues,

$$E_{1,2}(\mathbf{k})=\left[\zeta_{\mathbf{k}}^2\pm2\sqrt{E_{0,\mathbf{k}}^2h_{\mathbf{k}}^2-\left(\frac{\kappa k_x}{m}\right)^2|\Delta_0|^2}\right]^{1/2}, \tag{13}$$

describe quasiparticle excitations, with the plus (+) associated with E_1 and the minus (−) with E_2. The second set of eigenvalues, $E_{3,4}(\mathbf{k})=-E_{2,1}(\mathbf{k})$, corresponds to quasiholes. Further, $\zeta_{\mathbf{k}}^2=E_{0,\mathbf{k}}^2+h_{\mathbf{k}}^2$, where $E_{0,\mathbf{k}}=\sqrt{\xi_{\mathbf{k}}^2+|\Delta_0|^2}$, and $h_{\mathbf{k}}=\sqrt{(\kappa k_x/m)^2+\Omega_R^2/4}$ is the magnitude of the combined spin-orbit and Rabi couplings.

We express the two-body interaction parameter g in terms of the renormalized s-wave scattering length a_s via the relation [51]

$$\frac{1}{g}=-\frac{m}{4\pi a_s}+\frac{1}{V}\sum_{\mathbf{k}}\frac{1}{2\varepsilon_{\mathbf{k}}}. \tag{14}$$

Note that a_s is the s-wave scattering length *in the absence of* spin-orbit and Rabi fields. It is, of course, possible to express g, and all subsequent relations, in terms of a scattering length which is renormalized by the presence of the spin-orbit and Rabi fields [53,54], but for both simplicity and the sake of referring to the more experimentally accessible quantity, we do not do so here.

The order-parameter equation is obtained from the saddle-point condition $\delta\Omega_0/\delta\Delta_0^*|_{T,V,\mu}=0$, leading to

$$\frac{m}{4\pi a_s}=\frac{1}{2V}\sum_{\mathbf{k}}\left[\frac{1}{\varepsilon_{\mathbf{k}}}-A_+(\mathbf{k})-\frac{\Omega_R^2}{4\xi_{\mathbf{k}}h_{\mathbf{k}}}A_-(\mathbf{k})\right], \tag{15}$$

where we introduced the notation

$$A_\pm(\mathbf{k})=\frac{1-2n_1(\mathbf{k})}{2E_1(\mathbf{k})}\pm\frac{1-2n_2(\mathbf{k})}{2E_2(\mathbf{k})}, \tag{16}$$

with $n_j(\mathbf{k})=1/[e^{\beta E_j(\mathbf{k})}+1]$ being the Fermi function. In addition, the particle number at the saddle point $N_0=-\partial\Omega_0/\partial\mu|_{T,V}$ is given by

$$N_0=\sum_{\mathbf{k}}\left\{1-\xi_{\mathbf{k}}\left[A_+(\mathbf{k})+\frac{(\kappa k_x/m)^2}{\xi_{\mathbf{k}}h_{\mathbf{k}}}A_-(\mathbf{k})\right]\right\}. \tag{17}$$

The mean-field temperature T_0 is determined by solving Eq. (15) for the given μ. The corresponding number of particles is given by Eq. (17). This mean-field treatment leads to a transition temperature $\sim e^{1/k_Fa_s}$, where k_F is the Fermi momentum. This result gives the correct transition temperature on the BCS limit; however, it is unphysical on the BEC regime for $k_Fa_s\to0$. In order to find a physical result, we need to include order-parameter fluctuations, which we now do.

B. Gaussian fluctuations

In discussing Gaussian fluctuations, we concentrate on equal Rasha-Dresselhaus couplings, leaving details for general Rashba-Dresselhaus coupling to Appendix C.

To obtain the correct superfluid transition temperature in the BEC limit, we must include the physics of two-body

bound states near the transition, as described by the two-particle T matrix [55,56]. Accounting for all two-particle channels, the T-matrix calculation leads to a two-particle scattering amplitude Γ, where

$$\Gamma^{-1}(\mathbf{q},z)=\frac{m}{4\pi a_s}-\frac{1}{2V}\sum_{\mathbf{k}}\left[\frac{1}{\varepsilon_{\mathbf{k}}}+\sum_{i,j=1}^{2}\alpha_{ij}W_{ij}\right]; \quad (18)$$

z is the complex frequency and

$$W_{ij}=\frac{1-n_i(\mathbf{k})-n_j(\mathbf{k}+\mathbf{q})}{z-E_i(\mathbf{k})-E_j(\mathbf{k}+\mathbf{q})}. \quad (19)$$

At the superfluid phase boundary $\Delta_0\to 0$, the eigenvalues appearing in Eq. (19) reduce to $E_{1,2}(\mathbf{k})=||\xi_{\mathbf{k}}|\pm h_{\mathbf{k}}|$, but it is straightforward to show that ignoring the absolute values does not result in any change in either the mean-field order parameter or number equation. Meanwhile, the coefficients

$$\alpha_{11}=\alpha_{22}=|u_{\mathbf{k}}u_{\mathbf{k}+\mathbf{q}}-v_{\mathbf{k}}v^{*}_{\mathbf{k}+\mathbf{q}}|^2, \quad (20)$$

$$\alpha_{12}=\alpha_{21}=|u_{\mathbf{k}}v_{\mathbf{k}+\mathbf{q}}+u_{\mathbf{k}+\mathbf{q}}v_{\mathbf{k}}|^2 \quad (21)$$

are the coherence factors associated with the quasiparticle amplitudes for $\Delta_0=0$:

$$u_{\mathbf{k}}=\sqrt{\frac{1}{2}\left(1+\frac{\Omega_R}{2h_{\mathbf{k}}}\right)},\quad v_{\mathbf{k}}=i\sqrt{\frac{1}{2}\left(1-\frac{\Omega_R}{2h_{\mathbf{k}}}\right)}. \quad (22)$$

The Gaussian fluctuation correction to the thermodynamic potential is

$$\Omega_F=-T\sum_{\mathbf{q},iq_n}\ln\left[\beta\Gamma(\mathbf{q},iq_n)/V\right] \quad (23)$$

over the entire BCS-to-BEC evolution. The fluctuation contribution to the particle number is therefore $N_F=-\partial\Omega_F/\partial\mu|_{T,V}$, where

$$N_F=\sum_{\mathbf{q}}\int_{-\infty}^{\infty}\frac{d\omega}{\pi}n_B(\omega)\left[\frac{\partial\delta(\mathbf{q},\omega)}{\partial\mu}-\frac{\partial\delta(\mathbf{q},0)}{\partial\mu}\right]_{T,V}, \quad (24)$$

with the phase shift $\delta(\mathbf{q},\omega)$ defined via the relation

$$\Gamma(\mathbf{q},\omega\pm i\epsilon)=|\Gamma(\mathbf{q},\omega)|e^{\pm i\delta(\mathbf{q},\omega)}. \quad (25)$$

When two-body states are present, the fluctuation contribution can be written as $N_F=N_{sc}+N_b$, where

$$N_{sc}=\sum_{\mathbf{q}}\int_{\omega_{tp}(\mathbf{q})}^{\infty}\frac{d\omega}{\pi}n_B(\omega)\left[\frac{\partial\delta(\mathbf{q},\omega)}{\partial\mu}-\frac{\partial\delta(\mathbf{q},0)}{\partial\mu}\right]_{T,V} \quad (26)$$

is the number of particles in scattering states, and $\omega_{tp}(\mathbf{q})$ is the two-particle continuum threshold corresponding to the branch point of $\Gamma^{-1}(\mathbf{q},z)$ [55,57],

$$N_b=2\sum_{\mathbf{q}}n_B[E_{bs}(\mathbf{q})-2\mu] \quad (27)$$

is the number of fermions in bound states, where $n_B(\omega)=1/(e^{\beta\omega}-1)$ is the Bose distribution function, and $E_{bs}(\mathbf{q})$ is the energy of the bound states obtained from $\Gamma^{-1}(\mathbf{q},z=E-2\mu)=0$, corresponding to a pole in the scattering amplitude $\Gamma(\mathbf{q},z)$. In the limit of large and negative fermion chemical potential, the system becomes nondegenerate and $\Gamma^{-1}(\mathbf{q},z)=0$ becomes the exact eigenvalue equation for the two-body bound state in the presence of spin-orbit and Rabi coupling [23]. The total number of fermions, as a function of μ, thus becomes

$$N=N_0+N_F, \quad (28)$$

where N_0 is given in Eq. (17) and N_F is the sum of N_{sc} and N_b, as discussed above [51,55].

IV. CRITICAL TEMPERATURE

We calculate numerically the transition temperature T_c between the normal and uniform superfluid states, as a function of the scattering parameter $1/k_Fa_s$, by simultaneously solving the order-parameter and number equations (15) and (28). The solutions correspond to the minima of the free energy, $\mathcal{F}=\Omega+\mu N$. We do not discuss the cases of Fulde-Ferrell [58] or Larkin-Ovchinnikov [59] nonuniform superfluid phases since they only exist over a very narrow region of the phase diagram deep in the BCS regime [58,59], which is not experimentally accessible for ultracold fermions.

Figure 1, in which we scale temperatures by the Fermi temperature $T_F=k_F^2/2m$, shows the effects of spin-orbit and Rabi couplings on T_c. The solid (black) line in Fig. 1(a) shows T_c versus $1/k_Fa_s$ for zero Rabi coupling ($\Omega_R=0$) and zero spin-orbit coupling κ. If $\Omega_R=0$, the spin-orbit coupling can be removed by a simple gauge transformation, and thus plays no role. In this situation, the pairing is purely s-wave. The dashed (blue) line shows T_c for $\Omega_R\neq 0$, with vanishing equal Rashba-Dresselhaus spin-orbit coupling. We see that for fixed interaction strength, the pair-breaking effect of the Rabi coupling suppresses superfluidity, compared with $\Omega_R=0$; the Rabi field here plays the pair-breaking role of the Zeeman field in a superconductor.

With both spin-orbit and Rabi couplings present, the two-particle pairing is no longer purely singlet s-wave, but obtains a triplet p-wave component; the admixture stabilizes the superfluid phase, as shown by the dotted (green) line. The latter curve shows that in the BEC regime with large positive $1/k_Fa_s$, the superfluid transition temperature is enhanced by the presence of spin-orbit and Rabi couplings, a consequence of the reduction of the bosonic effective mass in the x direction below $2m$. However, for sufficiently large Ω_R, the geometric mean bosonic mass M_B increases above $2m$ and T_c decreases. This renormalization of the mass of the bosons can be traced back to a change in the energy dispersion of the fermions when both spin-orbit coupling and Rabi fields are present.

Figure 1(b) shows T_c versus Ω_R for fixed $1/k_Fa_s$, both with and without equal Rashba-Dresselhaus spin-orbit coupling at $\kappa=0.5k_F$. When both κ and T are zero, superfluidity is destroyed at a critical value of Ω_R corresponding to the Clogston limit [60]. At low temperature, the phase transition to the normal state is first-order because the Rabi coupling is sufficiently large to break singlet Cooper pairs. However, at higher temperatures, the singlet s-wave superfluid starts to become polarized by thermally excited quasiparticles that produce a paramagnetic response. Thus, above the characteristic temperature indicated by the large (red) dots, the transition becomes second-order, as pointed out by Sarma [61]. The change in the transition order occurs not only for $\kappa=0$, but also for nonzero values of κ both in the BCS regime and near

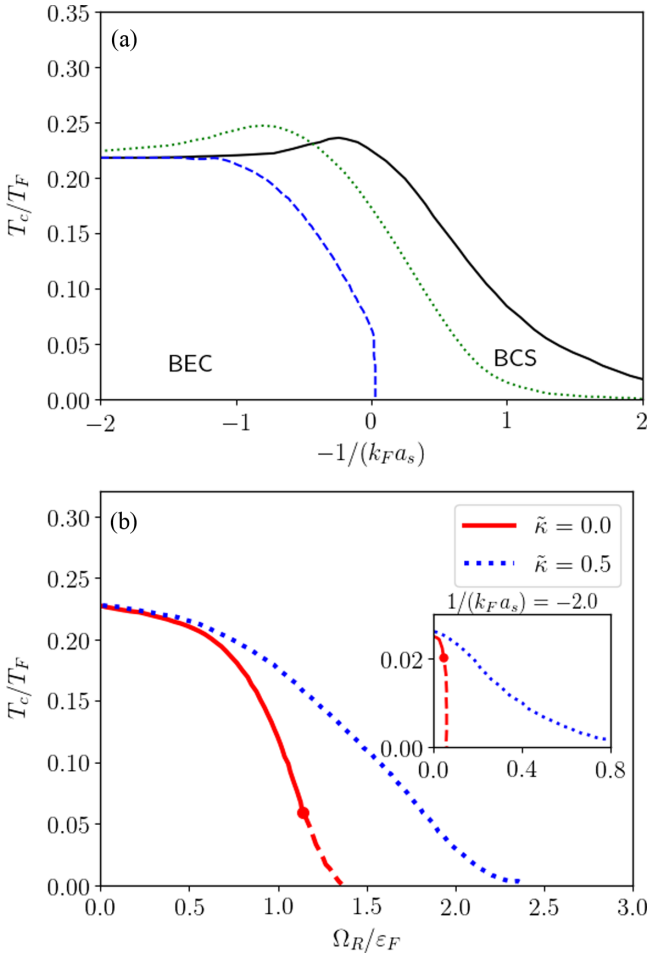

FIG. 1. (a) The superfluid transition temperature T_c/T_F, where T_F is the Fermi temperature, vs the scattering parameter $1/k_F a_s$ for equal Rashba-Dresselhaus spin-orbit coupling and two different Rabi coupling strengths, $\Omega_R = 0$ and ε_F. For $\Omega_R = 0$ [solid (black) curve], T_c is the same as for zero spin-orbit coupling since the equal spin-orbit field can be gauged away. The dashed (blue) line shows T_c for zero spin-orbit coupling, with $\Omega_R = \varepsilon_F$, while the dotted (green) line shows T_c for $\Omega_R = \varepsilon_F$ and $\tilde{\kappa} = \kappa/k_F = 0.5$. (b) T_c is drawn at unitarity, $1/k_F a_s = 0$, and in the inset at $1/k_F a_s = -2.0$, as a function of $\widetilde{\Omega}_R = \Omega_R/\varepsilon_F$. The solid (red) curves represent $\tilde{\kappa} = 0$ and the dotted (blue) curves represent $\tilde{\kappa} = 0.5$. Across the dotted (red) curves, the phase transition is first-order.

unitarity, depending on the choice of parameters, as illustrated in Fig. 1(b).

The critical temperature for $\kappa \neq 0$ vanishes only asymptotically in the limit of large Ω_R. We note that for $\Omega_R = E_F$ and $\kappa = 0$, the transition from the superfluid to the normal state is continuous at unitarity, but very close to a discontinuous transition. In the range $1.05 \lesssim \Omega_R/E_F \lesssim 1.10$, numerical uncertainties as $\kappa \to 0$ prevent us from predicting exactly whether the transition at unitarity is continuous or discontinuous.

Figure 2 shows $\mu(T_c)$ for fixed spin-orbit coupling and several Rabi couplings. The solid (black) curve, which represents the situation in which no Rabi field is present, is equivalent to the situation in which spin-orbit coupling is also absent, as noted in the discussion of Fig. 1. It is evident that while

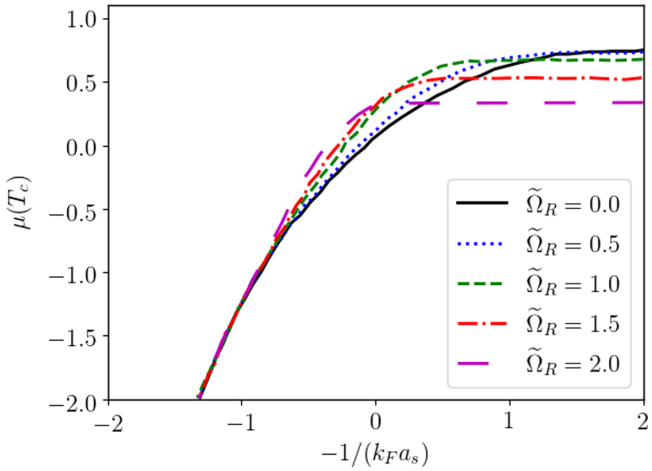

FIG. 2. Chemical potential at the superfluid critical temperature (T_c) for $\tilde{\kappa} = \kappa/k_F = 0.5$ and various Rabi fields, $\widetilde{\Omega}_R = \Omega_R/\varepsilon_F$.

the Rabi field reduces the chemical potential in the BCS limit, it also shifts the onset of the system's evolution to the BEC limit to larger inverse scattering lengths, and produces a nonmonotonic behavior of $\mu(T_c)$ near unitarity.

Figure 3 shows T_c for equal Rashba-Dresselhaus coupling $\kappa = 0.5 k_F$, as a function of Rabi field and scattering parameter. We also superpose the zero-temperature phase diagram to illustrate the different superfluid ground states of this system. According to the zeros of the lowest quasiparticle energy $E_2(\mathbf{k})$, the uniform superfluid phases that emerge are [21] direct gapped with zero rings (line nodes), indirectly gapped with zero rings, gapless with one ring, and gapless with two rings.

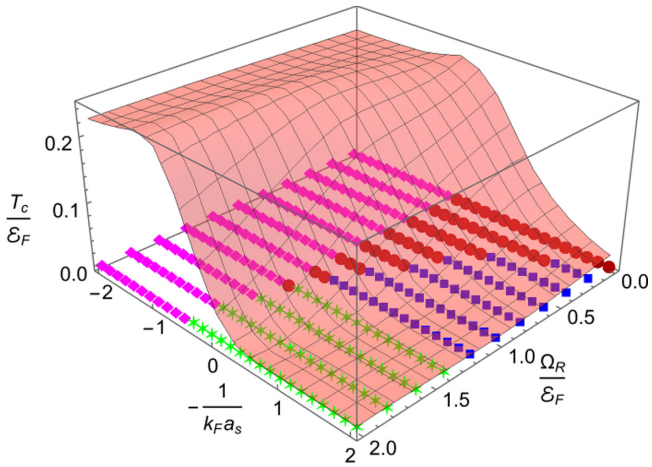

FIG. 3. Phase diagram of critical temperature T_c/T_F vs $1/k_F a_s$ and Ω_R/ε_F for equal Rashba-Dresselhaus coupling $\kappa/k_F = 0.5$. The finite-temperature uniform superfluid phases reflect those at $T = 0$ shown in the background. These phases are distinguished by the number of rings (line nodes) in the quasiparticle excitation spectrum [i.e., where $E_2(\mathbf{k}) = 0$] and type of gap: (1) direct gapped superfluid with zero rings (magenta diamonds), (2) indirect gapped superfluid with zero rings (red circles), (3) gapless superfluid with two rings (blue square), and (4) gapless one-ring superfluid (green stars).

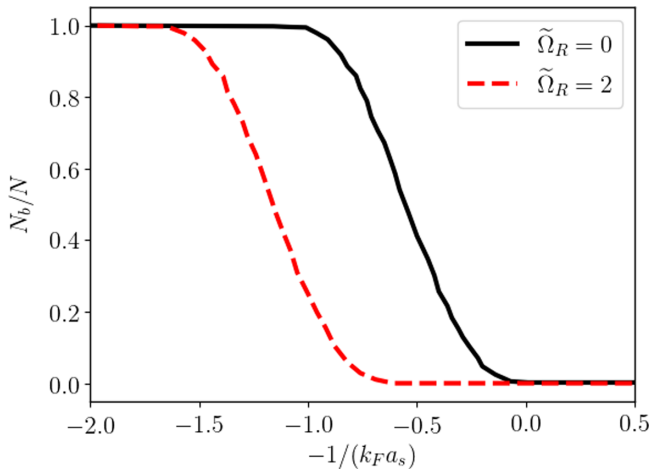

FIG. 4. Fractional number N_b/N of bound fermions as a function of the interaction parameter $1/k_F a_s$, for equal Rashba-Dresselhaus coupling $\kappa/k_F = 0.5$ and Rabi frequencies $\widetilde{\Omega}_R = \Omega_R/\varepsilon_F = 0$ (black solid line) and $\widetilde{\Omega}_R = \Omega_R/\varepsilon_F = 2$ (red dot-dashed line).

Figure 4 shows the fractional number N_b/N of bound fermions at T_c as a function of $1/k_F a_s$ for two sets of external fields. In the BCS (BEC) regime, the relative contribution to N is dominated by unbound (bound) fermions. The main effect of spin-orbit and Rabi fields on N_b/N is to shift the location where the two-body bound states emerge. For fixed spin-orbit coupling (Rabi field) and increasing Rabi field (spin-orbit coupling), two-body bound states emerge at larger (smaller) scattering parameters. These shifts are in agreement with the calculated shifts in binding energies of Feshbach molecules in the presence of equal Rashba-Dresselhaus spin-orbit coupling and Rabi fields [23].

V. GINZBURG-LANDAU THEORY

To further elucidate the effects of fluctuations on the order of the superfluid transition, as well as to assess the impact of spin-orbit and Rabi couplings near the critical temperature, we now derive the Ginzburg-Landau description of the free energy near the transition. In the limit of small order parameter, the fluctuation action $\mathcal{S}_F$ can be expanded in powers of the order parameter $\Delta(q)$ beyond Gaussian order. The expansion of $\mathcal{S}_F$ to quartic order is sufficient to describe the continuous (second-order) transition in T_c versus $1/k_F a_s$ in the absence of a Rabi field [51]. However, to correctly describe the first-order transition [60,61] at low temperature (Fig. 1), it is necessary to expand the free energy to sixth order in Δ.

The quadratic (Gaussian-order) term in the action is

$$\mathcal{S}_G = \beta V \sum_q \frac{|\Delta_q|^2}{\Gamma(\mathbf{q}, z)}. \tag{29}$$

For an order parameter varying slowly in space and time, we may expand Γ^{-1} as

$$\Gamma^{-1}(\mathbf{q}, z) = a + \sum_\ell c_\ell \frac{q_\ell^2}{2m} - d_0 z + \cdots, \tag{30}$$

with the sum over $\ell = \{x, y, z\}$. The full result, as a functional of $\Delta(\mathbf{r}, \tau)$, has the form

$$\mathcal{S}_F = \int_0^\beta d\tau \int d^3\mathbf{r} \Bigg(d_0 \Delta^* \frac{\partial}{\partial \tau} \Delta + a|\Delta|^2 + \sum_\ell c_\ell \frac{|\nabla_\ell \Delta|^2}{2m} + \frac{b}{2}|\Delta|^4 + \frac{f}{3}|\Delta|^6 \Bigg). \tag{31}$$

The full time-dependent Ginzburg-Landau action describes systems in and near equilibrium (e.g., with collective modes). The imaginary part of d_0 measures the nonconservation of $|\Delta|^2$ in time (i.e., the Cooper pair lifetime). Details of the derivation of $\mathcal{S}_F$ are found in Appendix D.

We are interested in systems at thermodynamic equilibrium, where the order parameter is independent of time, that is, $\Delta(\mathbf{r}, \tau) = \Delta(\mathbf{r})$. In this situation, minimizing the free energy $T\mathcal{S}_F$ with respect to Δ^* yields the Ginzburg-Landau equation,

$$\left[-\sum_\ell c_\ell \frac{\nabla_\ell^2}{2m} + b|\Delta(\mathbf{r})|^2 + f|\Delta(\mathbf{r})|^4 + a \right] \Delta(\mathbf{r}) = 0. \tag{32}$$

For $b > 0$, the system undergoes a continuous phase transition when a changes sign. However, when $b < 0$, the system is unstable in the absence of f. For $b < 0$ and $a > 0$, a first-order phase transition occurs when $3b^2 = 16af$. Positive f stabilizes the system even when $b < 0$.

In the BEC regime, where d_0 is purely real, we define an effective bosonic wave function $\Psi(\mathbf{r}) = \sqrt{d_0}\Delta(\mathbf{r})$ to recast Eq. (32) in the form of the Gross-Pitaevskii equation for a dilute Bose gas,

$$\left[-\sum_\ell \frac{\nabla_\ell^2}{2M_\ell} + U_2|\Psi(\mathbf{r})|^2 + U_3|\Psi(\mathbf{r})|^4 - \mu_B \right] \Psi(\mathbf{r}) = 0. \tag{33}$$

Here, $\mu_B = -a/d_0$ is the bosonic chemical potential, $M_\ell = m(d_0/c_\ell)$ are the anisotropic bosonic masses, and $U_2 = b/d_0^2$ and $U_3 = f/d_0^3$ represent contact interactions of two and three bosons. In the BEC regime, these terms are always positive, leading to a dilute gas of stable bosons. The boson chemical potential μ_B is $\approx 2\mu + E_b < 0$, where $E_b = -E_{bs}(\mathbf{q} = \mathbf{0})$ is the two-body binding energy in the presence of spin-orbit coupling and Rabi frequency, obtained from the condition $\Gamma^{-1}(\mathbf{q}, E - 2\mu) = 0$, discussed earlier.

The anisotropy of the effective bosonic masses, $M_x \neq M_y = M_z \equiv M_\perp$, stems from the anisotropy of the equal Rashba-Dresselhaus spin-orbit coupling, which together with the Rabi coupling modifies the dispersion of the constituent fermions along the x direction. In the limit $k_F a_s \ll 1$, the many-body effective masses reduce to those obtained by expanding the two-body binding energy, $E_{bs}(\mathbf{q}) \approx -E_b + \sum_\ell q_\ell^2/2M_\ell$, and agree with known results [23]. However, for $1/k_F a_s \lesssim 2$, many-body and thermal effects produce deviations from the two-body result.

In the absence of two- and three-body boson-boson interactions, U_2 and U_3, we directly obtain an analytic expression for T_c in the Bose limit from Eq. (27),

$$T_c = \frac{2\pi}{M_B} \left(\frac{n_B}{\zeta(3/2)} \right)^{2/3}, \tag{34}$$

with $M_B = (M_x M_\perp^2)^{1/3}$, by noting that $\mu_B = 0$ or $E_{bs}(\mathbf{q} = \mathbf{0}) - 2\mu = 0$, and using the condition that $n_B \simeq n/2$ [with corrections exponentially small in $(1/k_F a_s)^2$], where n_B is the density of bosons. In the BEC regime, the results shown in Fig. 1 include the effects of the mass anisotropy, but do not include the effects of boson-boson interactions.

To account for boson-boson interactions, we adopt the Hamiltonian of Eq. (33) with $U_2 \neq 0$, but with $U_3 = 0$, and apply the method developed in Ref. [62] to show that these interactions further increase T_{BEC} to

$$T_c(a_B) = (1 + \gamma) T_{BEC}, \tag{35}$$

where $\gamma = \lambda n_B^{1/3} a_B$. Here, a_B is the s-wave boson-boson scattering length, λ is a dimensionless constant ~ 1, and we use the relation $U_2 = 4\pi a_B / M_B$. Since $n_B = k_F^3/6\pi^2$ and the boson-boson scattering length is $a_B = U_2 M_B / 4\pi$, we have $\gamma = \tilde{\lambda} \widetilde{M}_B \widetilde{U}_2$, where $\widetilde{M}_B = M_B/2m$, $\widetilde{U}_2 = U_2 k_F^3/\varepsilon_F$, and $\tilde{\lambda} = \lambda/4(6\pi^5)^{1/3} \approx \lambda/50$. For fixed $1/k_F a_s$, T_c is enhanced by the spin-orbit field, a Ω_R-dependent decrease in the effective boson mass M_B ($\sim$10–15%), as well as a stabilizing boson-boson repulsion U_2 ($\sim$2–3%), for the parameters used in Fig. 1.

In closing our discussion of the strongly bound BEC limit, we note that in the absence of spin-orbit coupling, a Gaussian-order calculation of the two-boson scattering length yields the erroneous Born approximation result $a_B = 2a_s$. However, an analysis of the T matrix beyond Gaussian order, which includes the effects of two-body bound states, obtains the correct result $a_B = 0.6 a_s$ at very low densities [63] and agrees with four-body calculations [64]. The same method can be used to estimate U_2 or a_B beyond the Born approximation discussed above. Nevertheless, while the precise quantitative relation between a_B and a_s in the presence of spin-orbit coupling is yet unknown, the trend of increasing T_c due to spin-orbit coupling has been clearly shown.

VI. COMPARISON TO EARLIER WORK

In this section, we briefly compare our results with earlier investigations of different types of theoretically motivated spin-orbit couplings, worked in different dimensions or at zero temperature. Our results focus mainly on an analysis of the critical superfluid temperature and the effects thereon of order-parameter fluctuations for a three-dimensional Fermi gas in the presence of equal Rashba-Dresselhaus spin-orbit coupling and Rabi fields. The Appendices consider the more general situation of arbitrary Rashba and Dresselhaus components.

Several works have analyzed the effects of spin-orbit-coupled fermions in three dimensions at zero temperature [17–22,65–68]. While some authors have described the situation of Rashba-only couplings [17–19,65], others have assessed the case of equal Rashba and Dresselhaus components [21,22] or a general mixture of the two [20]. It has been demonstrated that in the absence of a Rabi field, the zero-temperature evolution from BCS to BEC superfluidity is a crossover for s-wave systems, not only for Rashba-only couplings [17–20,65], but also for arbitrary Rashba and Dresselhaus components [20]. This result directly follows from the fact that the quasiparticle excitation spectrum remains fully gapped throughout the evolution.

In contrast, the addition of a Rabi field gives rise to topological phase transitions for Rashba-only couplings [17] and equal Rashba and Dresselhaus components [21,22], a situation which certainly persists for general Rashba-Dresselhaus couplings. The simultaneous presence of a general Rashba-Dresselhaus spin-orbit coupling and Rabi fields leads to a qualitative change in the quasiparticle excitation spectrum and to the emergence of topological superfluid phases [17,21,22]. Two-dimensional systems have also been investigated at zero temperature, where topological phase transitions have been identified for Rashba-only [69] and equal Rashba-Dresselhaus [70] couplings, in the presence of a Rabi field.

While early papers in this field focused mainly on the zero-temperature limit, progress toward finite-temperature theories was made first in two dimensions [71,72] and later in three dimensions [73–75]. The effects of a general Rashba-Dresselhaus spin-orbit coupling and Rabi field on the Berezenskii-Kosterlitz-Thouless transition were thoroughly investigated for two-dimensional Fermi gases at finite temperatures [71,72], including both Rashba-only and equal Rashba-Dresselhaus spin-orbit couplings as examples.

The superfluid critical temperature in three dimensions was investigated using a spherical (3D) spin-orbit coupling $\lambda \mathbf{k} \cdot \boldsymbol{\sigma}$ in the absence of a Rabi field [73,74], and also for Rashba-only (2D) couplings in the presence of a Rabi field [75]. In a recent review article [76], the critical temperature throughout the BCS-BEC evolution was discussed both in the absence [51] and presence [52] of Rashba-Dresselhaus spin-orbit coupling. In Secs. 5 and 6 of this review, the authors describe the same method and expressions we obtained in our earlier preliminary work [52] for the analytical relations required to obtain the critical temperature at the Gaussian order; they include, however, only the contribution of bound states discussed earlier in the literature for Rashba-only spin-orbit coupling without Rabi fields [18]. In contrast, here we develop a complete Gaussian theory to compute the superfluid critical temperature of a three-dimensional Fermi gas in the presence of both a general Rashba-Dresselhaus (2D) spin-orbit coupling and Rabi fields. We focus our numerical calculations on the specific situation of equal Rashba-Dresselhaus components, which is easier to achieve experimentally in the context of ultracold atoms. Our key results, already announced in our earlier work [52], include the contributions of bound and scattering states at the Gaussian level. As seen in Fig. 4 of this present paper, there is a wide region of interaction parameters for which the contribution of scattering states cannot be neglected. Furthermore, unlike previous work [73–76], we provide a comprehensive analysis of the Ginzburg-Landau fluctuation theory and include the effects of boson-boson interactions on the superfluid critical temperature in the BEC regime.

VII. CONCLUSION

We have evaluated the superfluid critical temperature throughout the BCS-to-BEC evolution of three-dimensional Fermi gases in the presence of equal Rashba-Dresselhaus spin-orbit couplings, Rabi fields, and tunable s-wave interactions. Furthermore, we have developed the Ginzburg-Landau theory up to sixth power in the order parameter to elucidate the

origin of first-order phase transitions when the spin-orbit field is absent and the Rabi field is sufficiently large. Lastly, in the Appendices, we have presented the finite-temperature theory of s-wave interacting fermions in the presence of a generic Rashba-Dresselhaus coupling and external Rabi fields, as well as the corresponding time-dependent Ginzburd-Landau theory near the superfluid critical temperature.

ACKNOWLEDGMENTS

We thank I. B. Spielman for discussions. The research of P.D.P. was supported in part by NSF Grant No. PHY1305891 and that of G.B. by NSF Grants No. PHY1305891 and No. PHY1714042. Both G.B. and C.A.R.SdM. thank the Aspen Center for Physics, supported by NSF Grants No. PHY1066292 and No. PHY1607611, where part of this work was done. This work was performed under the auspices of the U.S. Department of Energy by Lawrence Livermore National Laboratory under Contract No. DE-AC52-07NA27344.

APPENDIX A: HAMILTONIAN AND EFFECTIVE LAGRANGIAN FOR GENERAL RASHBA-DRESSELHAUS SPIN-ORBIT COUPLING

In this Appendix, we consider a larger class of spin-coupled fermions in three dimensions with a general Rashba-Dresselhaus (GRD) coupling. The Hamiltonian density for equal Rashba-Dresselhaus (ERD) discussed in Sec. II is a particular case of the general Rashba-Dresselhaus Hamiltonian density,

$$\mathcal{H}(\mathbf{r}) = \mathcal{H}_0(\mathbf{r}) + \mathcal{H}_{\rm so}(\mathbf{r}) + \mathcal{H}_I(\mathbf{r}). \tag{A1}$$

Adopting units in which $\hbar = k_B = 1$, the independent-particle Hamiltonian density without spin-orbit coupling is

$$\mathcal{H}_0(\mathbf{r}) = \sum_\alpha \left[\frac{|\nabla\psi_\alpha(\mathbf{r})|^2}{2m_\alpha} - \mu_\alpha \psi_\alpha^\dagger(\mathbf{r})\psi_\alpha(\mathbf{r}) \right], \tag{A2}$$

where ψ_α, m_α, and μ_α are the fermion field operator, mass, and chemical potentials for internal state α, respectively. The spin-orbit Hamiltonian can be written as

$$\mathcal{H}_{\rm so}(\mathbf{r}) = -\sum_{i\alpha\beta} \psi_\alpha^\dagger(\mathbf{r})\sigma_{i,\alpha\beta} h_i(\mathbf{r})\psi_\beta(\mathbf{r}), \tag{A3}$$

where the $\boldsymbol{\sigma}_i$ are the Pauli matrices in isospin (internal state) space and $\mathbf{h} = (h_x, h_y, h_z)$ includes both the spin-orbit coupling and Zeeman fields. Finally, we consider a two-body s-wave contact interaction,

$$\mathcal{H}_I(\mathbf{r}) = -g\psi_\uparrow^\dagger(\mathbf{r})\psi_\downarrow^\dagger(\mathbf{r})\psi_\downarrow(\mathbf{r})\psi_\uparrow(\mathbf{r}), \tag{A4}$$

where $g > 0$ corresponds to an attractive interaction.

By introducing the pairing field $\Delta(\mathbf{r},\tau) = -g\langle\psi_\downarrow(\mathbf{r},\tau)\psi_\uparrow(\mathbf{r},\tau)\rangle$, we remove the quartic interaction and obtain the Lagrangian density,

$$\mathcal{L}(\mathbf{r},\tau) = \frac{1}{2}\Psi^\dagger(\mathbf{r},\tau)\mathbf{G}^{-1}(\hat{\mathbf{k}},\tau)\Psi(\mathbf{r},\tau) + \frac{|\Delta(\mathbf{r},\tau)|^2}{g} + \widetilde{K}_+(\hat{\mathbf{k}})\delta(\mathbf{r}-\mathbf{r}'), \tag{A5}$$

where we introduced the momentum operator $\hat{\mathbf{k}} = -i\nabla$, the Nambu spinor $\Psi = (\psi_\uparrow\psi_\downarrow\psi_\uparrow^\dagger\psi_\downarrow^\dagger)^T$, and defined $\widetilde{K}_\pm = (\widetilde{K}_\uparrow \pm \widetilde{K}_\downarrow)/2$. Here, $\widetilde{K}_\uparrow = K_\uparrow - h_z$, and $\widetilde{K}_\downarrow = K_\downarrow + h_z$, with $K_\alpha(\hat{\mathbf{k}}) = \hat{\mathbf{k}}^2/(2m_\alpha) - \mu_\alpha$ being the kinetic energy operator of internal state α with respect to its chemical potential. Lastly, the inverse Green's operator appearing in Eq. (A5) is

$$\mathbf{G}^{-1}(\hat{\mathbf{k}},\tau) = \begin{pmatrix} \partial_\tau - \widetilde{K}_\uparrow & h_\perp^* & 0 & -\Delta \\ h_\perp & \partial_\tau - \widetilde{K}_\downarrow & \Delta & 0 \\ 0 & \Delta^* & \partial_\tau + \widetilde{K}_\uparrow & -h_\perp \\ -\Delta^* & 0 & -h_\perp^* & \partial_\tau + \widetilde{K}_\downarrow \end{pmatrix}, \tag{A6}$$

where $h_\perp(\hat{\mathbf{k}}) = h_x(\hat{\mathbf{k}}) + ih_y(\hat{\mathbf{k}})$ plays the role of the spin-orbit coupling, and h_z is the Zeeman field along the z direction.

To make progress, we expand the order parameter about its saddle-point (mean-field) value Δ_0 by writing $\Delta(\mathbf{r},\tau) = \Delta_0 + \eta(\mathbf{r},\tau)$. Next, we integrate over the fermionic fields and use the decomposition $\mathbf{G}^{-1}(\hat{\mathbf{k}},\tau) = \mathbf{G}_0^{-1}(\hat{\mathbf{k}},\tau) + \mathbf{G}_F^{-1}(\hat{\mathbf{k}},\tau)$, where $\mathbf{G}_0^{-1}(\hat{\mathbf{k}},\tau)$ is the mean-field Green's operator, given by Eq. (A6) with $\Delta(\mathbf{r},\tau) = \Delta_0$, and $\mathbf{G}_F^{-1}(\hat{\mathbf{k}},\tau)$ is the contribution to the inverse Green's operator arising from fluctuations. These steps yield the saddle-point Lagrangian density,

$$\mathcal{L}_0(\mathbf{r},\tau) = -\frac{T}{2V}\mathrm{Tr}\ln\left(\beta\mathbf{G}_0^{-1}\right) + \frac{|\Delta_0|^2}{g} + \widetilde{K}_+(\hat{\mathbf{k}})\delta(\mathbf{r}-\mathbf{r}'), \tag{A7}$$

and the fluctuation contribution,

$$\mathcal{L}_F(\mathbf{r},\tau) = -\frac{T}{2V}\mathrm{Tr}\ln\left(\mathbf{I} + \mathbf{G}_0\mathbf{G}_F^{-1}\right) + \Lambda(\mathbf{r},\tau) + \frac{|\eta(\mathbf{r},\tau)|^2}{g}, \tag{A8}$$

resulting in the effective Lagrangian density $\mathcal{L}_{\rm eff}(\mathbf{r},\tau) = \mathcal{L}_0(\mathbf{r},\tau) + \mathcal{L}_F(\mathbf{r},\tau)$. In the expressions above, we work in a volume V and take traces over both discrete and continuous indices. Notice that the term $\Lambda(\mathbf{r},\tau) = [\Delta_0\eta^*(\mathbf{r},\tau) + \Delta_0^*\eta(\mathbf{r},\tau)]/g$ in the fluctuation Lagrangian cancels out the linear terms in η and η^* when the logarithm is expanded, due to the saddle-point condition,

$$\frac{\delta S_0}{\delta\Delta_0^*} = 0, \tag{A9}$$

where $S_0 = \int_0^\beta d\tau d^3\mathbf{r}\mathcal{L}_0(\mathbf{r},\tau)$ is the saddle-point action.

APPENDIX B: SADDLE-POINT APPROXIMATION FOR GENERAL RASHBA-DRESSELHAUS SPIN-ORBIT COUPLING

We first analyze the saddle-point contribution. The saddle-point thermodynamic potential $\Omega_0 = -T\ln\mathcal{Z}_0$ can be obtained for the saddle-point partition function $\mathcal{Z} = e^{-S_0}$ as $\Omega_0 = TS_0$. Transforming the saddle-point Lagrangian $\mathcal{L}_0$ from Eq. (A7) into momentum space and integrating over spatial coordinates and imaginary time leads to the saddle-point thermodynamic potential,

$$\Omega_0 = V\frac{|\Delta_0|^2}{g} - \frac{T}{2}\sum_{\mathbf{k},j}\ln(1+e^{-\beta E_{\mathbf{k},j}}) + \sum_{\mathbf{k}}\widetilde{K}_+(\mathbf{k}), \tag{B1}$$

where $K_\alpha(\mathbf{k}) = \mathbf{k}^2/2m_\alpha - \mu_\alpha$ and the eigenvalues $E_{\mathbf{k},j}$ are the poles of $\mathbf{G}_0(\mathbf{k},z)$, with $j = \{1,2,3,4\}$.

Next, we restrict our analysis to mass balanced systems ($m_\uparrow = m_\downarrow$) in diffusive equilibrium ($\mu_\uparrow = \mu_\downarrow$). We also consider the general Rashba-Dresselhaus (GRD) spin-orbit field $h_\perp(\mathbf{k}) = \kappa(k_x + i\eta k_y)/m$, where κ and η are the magnitude and anisotropy of the spin-orbit coupling, respectively. Note that this form is equivalent to another common form of the Rashba-Dresselhaus coupling found in the literature [21,22]: $\mathbf{h}_{\rm so} = \mathbf{h}_R + \mathbf{h}_D$, where $\mathbf{h}_R = v_R(k_x\hat{\mathbf{y}} - k_y\hat{\mathbf{x}})$ and $\mathbf{h}_D = v_D(k_x\hat{\mathbf{y}} + k_y\hat{\mathbf{x}})$. The two forms are related via a momentum-space rotation and the correspondences $\kappa = m(v_R + v_D)$ and $\eta = (v_R - v_D)/(v_R + v_D)$. The equal Rashba-Dresselhaus limit (ERD) corresponds to $v_R = v_D = v$, leading to $\eta = 0$ and $\kappa = 2mv$. The specific case of equal Rashba-Dresselhaus spin-orbit coupling discussed in the main part of the paper corresponds to the case where $\eta = 0$, that is, $h_\perp(\mathbf{k}) = \kappa k_x/m$.

For the general Rashba-Dresselhaus case, the four eigenvalues are

$$E_{1,2}(\mathbf{k}) = \left[\zeta_{\mathbf{k}}^2 \pm 2\sqrt{E_{0,\mathbf{k}}^2 h_{\mathbf{k}}^2 - |\Delta_0|^2|h_\perp(\mathbf{k})|^2}\right]^{1/2}, \quad \text{(B2)}$$

$$E_{3,4}(\mathbf{k}) = -E_{2,1}(\mathbf{k}), \quad \text{(B3)}$$

where the $+$ $(-)$ sign within the outermost square root corresponds to E_1 (E_2), and the functions inside the square roots are $\zeta_{\mathbf{k}}^2 = E_{0,\mathbf{k}}^2 + h_{\mathbf{k}}^2$, with contributions

$$E_{0,\mathbf{k}} = \sqrt{\xi_{\mathbf{k}}^2 + |\Delta_0|^2}, \quad \text{(B4)}$$

$$h_{\mathbf{k}} = \sqrt{|h_\perp(\mathbf{k})|^2 + h_z^2}, \quad \text{(B5)}$$

where $\xi_{\mathbf{k}} = \varepsilon_{\mathbf{k}} - \mu$, and $\varepsilon_{\mathbf{k}} = \mathbf{k}^2/2m$. The order-parameter equation is found from the saddle-point condition $\delta\Omega_0/\delta\Delta_0^*|_{T,V,\mu} = 0$. At the phase boundary between the superfluid and normal phases, $\Delta_0 \to 0$, and the order-parameter equation becomes

$$\frac{m}{4\pi a_s} = \frac{1}{2V}\sum_{\mathbf{k}}\left[\frac{1}{\varepsilon_{\mathbf{k}}} - \frac{\tanh(\beta E_1/2)}{2E_1} - \frac{\tanh(\beta E_2/2)}{2E_2} - \frac{h_z^2}{\xi_{\mathbf{k}}h_{\mathbf{k}}}\left(\frac{\tanh(\beta E_1/2)}{2E_1} - \frac{\tanh(\beta E_2/2)}{2E_2}\right)\right], \quad \text{(B6)}$$

after expressing the interaction parameter g in terms of the s-wave scattering length via the relation

$$\frac{1}{g} = -\frac{m}{4\pi a_s} + \frac{1}{V}\sum_{\mathbf{k}}\frac{1}{2\varepsilon_{\mathbf{k}}}. \quad \text{(B7)}$$

We note that a_s is the s-wave scattering length *in the absence of* spin-orbit and Zeeman fields. It is, of course, possible to express all relations obtained in terms of a scattering length which is renormalized by the presence of the spin-orbit and Rabi fields [53,54]. However, in addition to complicating our already cumbersome expressions, it would make reference to a quantity that is more difficult to measure experimentally and that would hide the explicit dependence of the properties that we analyze in terms of the spin-orbit and Rabi fields, so we do not consider such complications here. Note that since $\Delta_0 = 0$ at the phase boundary, the eigenvalues in Eq. (B2) reduce to $E_1(\mathbf{k}) = ||\xi_{\mathbf{k}}| + h_{\mathbf{k}}|$, $E_2(\mathbf{k}) = ||\xi_{\mathbf{k}}| - h_{\mathbf{k}}|$, which is the absolute value of the normal-state energy dispersions. However, it is straightforward to show that ignoring the absolute values does not result in any change in either the mean-field order parameter given by Eq. (B6) or number equation shown in Eq. (B8), when $\Delta_0 \to 0$.

The saddle-point critical temperature T_0 is determined by solving Eq. (B6) subject to the thermodynamic constraint $N_0 = -\partial\Omega_0/\partial\mu|_{T,V}$, which yields

$$N_0 = \sum_{\mathbf{k}}\left\{1 - \xi_{\mathbf{k}}\left[\frac{1}{\varepsilon_{\mathbf{k}}} + \frac{\tanh(\beta E_1/2)}{2E_1} + \frac{\tanh(\beta E_2/2)}{2E_2} + \frac{|h_\perp(\mathbf{k})|^2}{\xi_{\mathbf{k}}h_{\mathbf{k}}}\left(\frac{\tanh(\beta E_1/2)}{2E_1} - \frac{\tanh(\beta E_2/2)}{2E_2}\right)\right]\right\}. \quad \text{(B8)}$$

A mean-field description of the system, which involves a simultaneous solution of Eqs. (B6) and (B8), yields the asymptotically correct description of the system in the BCS limit; however, such a description fails miserably in the BEC regime where it does not account for the formation of two-body bound states. The general Rashba-Dresselhaus spin-orbit saddle-point equations (B6) and (B8) reduce to the equal Rashba-Dresselhaus equations (15) and (17) of the main part of the paper with the explicit use of $h_z = \Omega_R/2$ and $h_\perp(\mathbf{k}) = \kappa k_x/m$, where Ω_R is the Rabi coupling.

APPENDIX C: DERIVATION OF THE MODIFIED NUMBER EQUATION WITH GAUSSIAN FLUCTUATIONS

We begin by deriving the modified number equation arising from Gaussian fluctuations of the order parameter near the superfluid phase boundary. The fluctuation thermodynamic potential Ω_F results from the Gaussian integration of the fields $\eta(\mathbf{r}, \tau)$ and $\eta^*(\mathbf{r}, \tau)$ in the fluctuation partition function $\mathcal{Z}_F = \int d\eta^* d\eta e^{-S_F}$, where the action $S_F = \int d\tau_0^\beta \int d^3\mathbf{r}\mathcal{L}_F(\mathbf{r}, \tau)$ is calculated to quadratic order. The contribution to the thermodynamic potential due to Gaussian fluctuations is

$$\Omega_F = -T\sum_{iq_n,\mathbf{q}} \ln\left[\beta\Gamma(\mathbf{q}, iq_n)/V\right], \quad \text{(C1)}$$

where $q_n = 2\pi nT$ are the bosonic Matsubara frequencies and $\Gamma(\mathbf{q}, iq_n)$ is directly related to the pair fluctuation propagator $\chi_{pair}(\mathbf{q}, iq_n) = V\Gamma^{-1}(\mathbf{q}, iq_n)$.

The Matsubara sum can be evaluated via contour integration,

$$\Omega_F = -T\sum_{\mathbf{q}}\oint_{\mathcal{C}}\frac{dz}{2\pi i}n_B(z)\ln\left[\beta\Gamma(\mathbf{q}, z)/V\right], \quad \text{(C2)}$$

where $n_B(z) = 1/(e^z - 1)$ is the Bose function and the contour $\mathcal{C}$ encloses all of the Matsubara poles of the Bose function. Next, we deform the contour around the Matsubara frequencies towards infinity, taking into account the branch cut and the possibility of poles coming from the logarithmic term inside the contour integral. We take the branch cut to be along the real axis, then add and subtract the pole at $iq_n = 0$ to obtain

$$\Omega_F = -T\sum_{\mathbf{q}}\int_{-\infty}^{\infty}\frac{d\omega}{\pi}n_B(\omega)[\delta(\mathbf{q}, \omega) - \delta(\mathbf{q}, 0)], \quad \text{(C3)}$$

where the phase shift $\delta(\mathbf{q},\omega)$ is defined via $\Gamma(\mathbf{q},\omega\pm i\epsilon) = |\Gamma(\mathbf{q},\omega)|e^{\pm i\delta(\mathbf{q},\omega)}$, and arises from the contour segments above and below the real axis.

The thermodynamic identity $N = -\partial\Omega/\partial\mu|_{T,V}$ then yields to the fluctuation correction,

$$N_F = T\sum_{\mathbf{q}}\int_{-\infty}^{\infty}\frac{d\omega}{\pi}n_B(\omega)\left[\frac{\partial\delta(\mathbf{q},\omega)}{\partial\mu} - \frac{\partial\delta(\mathbf{q},0)}{\partial\mu}\right], \quad \text{(C4)}$$

to the the saddle-point number equation, and has a similar analytical structure as in the case without spin-orbit and Zeeman fields [51,55]. Thus, we can write the final number equation at the critical temperature T_c as $N = N_0 + N_F$. Since the phase shift $\delta(\mathbf{q},z)$ vanishes everywhere that $\Gamma(\mathbf{q},z)$ is analytic, the only contributions to Eq. (C4) arise from a possible isolated pole at $\omega_p(\mathbf{q})$ and a branch cut extending from the two-particle continuum threshold $\omega_{tp}(\mathbf{q}) = \min_{\{i,j,\mathbf{k}\}}[E_i(\mathbf{k}) + E_j(\mathbf{k}+\mathbf{q})]$ to $z\to\infty$ along the positive real axis. The explicit form of $\Gamma(\mathbf{q},z)$ can be extracted from Eq. (D15) of Appendix D.

When there is a pole corresponding to the emergence of a two-body bound state, we can explicitly write $\Gamma(\mathbf{q},z)\sim R(\mathbf{q})/[z-\omega_p(\mathbf{q})]$, from which we obtain $\partial\delta(\mathbf{q},\omega)/\partial\mu = 2\delta[z-\omega_p(\mathbf{q})]$, leading to the bound state density,

$$N_b = 2\sum_{\mathbf{q}} n_B(\omega_p(\mathbf{q})), \quad \text{(C5)}$$

where the energy $\omega_p(\mathbf{q})$ must lie below the two-particle continuum threshold $\omega_{tp}(\mathbf{q})$. The factor of 2, which arises naturally, is due to the two fermions comprising a bosonic molecule. Naturally, the presence of this term in the fluctuation-modified number equation is dependent upon the existence of such a pole, that is, a molecular bound state. These bound states correspond to the Feshbach molecules in the presence of spin-orbit coupling and Zeeman fields [7,23].

Having extracted the pole contribution to Eq. (C4), when it exists, the remaining integral over the branch cut corresponds to scattering state fermions,

$$N_{sc} = T\sum_{\mathbf{q}}\int_{\omega_{tp}(\mathbf{q})}^{\infty}\frac{d\omega}{\pi}n_B(\omega)\left[\frac{\partial\delta(\mathbf{q},\omega)}{\partial\mu} - \frac{\partial\delta(\mathbf{q},0)}{\partial\mu}\right], \quad \text{(C6)}$$

whose energy is larger than the minimum energy $\omega_{tp}(\mathbf{q})$ of two free fermions. Thus, when bound states are present, we arrive at the modified number equation,

$$N = N_0 + N_{sc} + N_b, \quad \text{(C7)}$$

where N_0 is the number of free fermions obtained from the saddle-point analysis in Eq. (B8), and N_b and N_{sc} are the bound state and scattering contributions given in Eqs. (C5) and (C6), respectively. These general results are particularized to the equal Rashba-Dresselhaus case in Sec. III B of this paper.

The number of unbound states N_u is then easily seen to be $N_u = N_0 + N_{sc}$, that is, the sum of the free-fermion (N_0) and scattering (N_{sc}) contributions. Naturally, the number of unbound states is also equal to the total number of states, N, minus the number of bound states, N_b, that is, $N_u = N - N_b$.

APPENDIX D: DERIVATION OF GINZBURG-LANDAU COEFFICIENTS FOR GENERAL RASHBA-DRESSELHAUS SPIN-ORBIT COUPLING

Next, we derive explicit expressions for the coefficients of the time-dependent Ginzburg-Landau theory valid near the critical temperature of the superfluid. We start from the fluctuation Lagrangian,

$$\mathcal{L}_F(\mathbf{r},\tau) = -\frac{T}{2V}\mathrm{Tr}\ln\left(\mathbf{I}+\mathbf{G}_0\mathbf{G}_F^{-1}\right) + \Lambda(\mathbf{r},\tau) + \frac{|\eta(\mathbf{r},\tau)|^2}{g}, \quad \text{(D1)}$$

in a volume V, and take the traces over both discrete and continuous indices. Notice that the term $\Lambda(\mathbf{r},\tau) = [\Delta_0\eta^*(\mathbf{r},\tau) + \Delta_0^*\eta(\mathbf{r},\tau)]/g$ in the fluctuation Lagrangian cancels out the linear terms in η and η^* when the logarithm is expanded, due to the saddle-point condition. Since the expansion is performed near T_c, we take the saddle-point order parameter $\Delta_0\to 0$ and redefine the fluctuation field as $\eta(\mathbf{r},\tau) = \Delta(\mathbf{r},\tau)$ to obtain

$$\mathcal{L}_F(\mathbf{r},\tau) = \frac{|\Delta|^2}{g} - \frac{T}{2V}\mathrm{Tr}\ln\left(\mathbf{I}+\mathbf{G}_0[0]\mathbf{G}_F^{-1}[\Delta]\right). \quad \text{(D2)}$$

Notice that the arguments in $\mathbf{G}_0[0]$ and $\mathbf{G}_F^{-1}[\Delta]$ represent the values of $\Delta_0 = 0$ and $\eta = \Delta$, respectively.

We expand the logarithm to sixth order in Δ to obtain

$$\mathcal{L}_F(\mathbf{r},\tau) = \frac{|\Delta|^2}{g} + \frac{T}{2V}\mathrm{Tr}\left[\frac{1}{2}\left(\mathbf{G}_0\mathbf{G}_F^{-1}\right)^2 + \frac{1}{4}\left(\mathbf{G}_0\mathbf{G}_F^{-1}\right)^4 + \frac{1}{6}\left(\mathbf{G}_0\mathbf{G}_F^{-1}\right)^6 + \cdots\right], \quad \text{(D3)}$$

where the higher-order odd (cubic and quintic) terms in the order-parameter amplitudes expansion can be shown to vanish due to conservation laws and energy or momentum considerations.

The traces can be evaluated explicitly by using the momentum-space inverse single-particle Green's function,

$$\mathbf{G}_0^{-1}(k,k') = \begin{pmatrix}\mathbf{A}^{-1}(k) & \mathbf{0}\\ \mathbf{0} & -[\mathbf{A}^{-1}(-k)]^T\end{pmatrix}\delta_{kk'}, \quad \text{(D4)}$$

derived from Eq. (A6). Here, we use the shorthand notation $k\equiv(i\omega,\mathbf{k})$, where $\omega_n = 2\pi nT$ are bosonic Matsubara frequencies and define the 2×2 matrix,

$$\mathbf{A}^{-1}(k) = \begin{pmatrix}i\omega_n - \widetilde{K}_\uparrow(\mathbf{k}) & h_\perp^*(\mathbf{k})\\ h_\perp(\mathbf{k}) & i\omega_n - \widetilde{K}_\downarrow(\mathbf{k})\end{pmatrix}, \quad \text{(D5)}$$

where $\widetilde{K}_\uparrow = \xi_{\mathbf{k}} - h_z$, $\widetilde{K}_\downarrow = \xi_{\mathbf{k}} + h_z$, with $\xi_{\mathbf{k}} = \mathbf{k}^2/2m - \mu$ the kinetic energy relative to the chemical potential, h_z the external Zeeman field, and $h_\perp(\mathbf{k}) = h_x(\mathbf{k}) + ih_y(\mathbf{k})$ the spin-orbit field. We also define the fluctuation contribution to the inverse Green's function,

$$\mathbf{G}_F^{-1}(k,k') = \begin{pmatrix}\mathbf{0} & -i\boldsymbol{\sigma}_y\Delta_{k-k'}\\ i\boldsymbol{\sigma}_y\Delta_{k'-k}^\dagger & \mathbf{0}\end{pmatrix}, \quad \text{(D6)}$$

where $\boldsymbol{\sigma}_y$ is the second Pauli matrix in isospin (internal state) space and

$$\Delta_k = \frac{\beta}{V}\int_0^\beta d\tau\int d^3\mathbf{r}e^{i(\mathbf{k}\cdot\mathbf{r}-\omega\tau)}\Delta(r) \quad \text{(D7)}$$

is the Fourier transform of $\Delta(r)$, with $r \equiv (\mathbf{r}, \tau)$, and also has dimensions of energy. Recall that we set $\hbar = k_B = 1$, such that energy, frequency, and temperature have the same units.

Inversion of Eq. (D4) yields

$$\mathbf{G}_0(k,k') = \begin{pmatrix} \mathbf{A}(k) & \mathbf{0} \\ \mathbf{0} & -[\mathbf{A}(-k)]^T \end{pmatrix} \delta_{kk'}, \tag{D8}$$

where the matrix $\mathbf{A}(k)$ is

$$\mathbf{A}(k) = \frac{1}{\det[\mathbf{A}^{-1}(k)]} \begin{pmatrix} i\omega_n - \widetilde{K}_{\downarrow}(\mathbf{k}) & -h_{\perp}^*(\mathbf{k}) \\ -h_{\perp}(\mathbf{k}) & i\omega_n - \widetilde{K}_{\uparrow}\mathbf{k}) \end{pmatrix}, \tag{D9}$$

with $\det[\mathbf{A}^{-1}(k)] = \prod_{j=1}^{2}[i\omega_n - E_j(\mathbf{k})]$ and where the independent-particle eigenvalues $E_j(\mathbf{k})$ are two of the poles of $\mathbf{G}_0(k,k)$. These poles are exactly the general eigenvalues described in Eqs. (B2) in the limit of $\Delta_0 \to 0$. Note that setting $\Delta_0 = 0$ in the general eigenvalue expressions yields $E_{1,2}(\mathbf{k}) = ||\xi_{\mathbf{k}}| \pm h_{\mathbf{k}}|$. The other set of poles of $\mathbf{G}_0(k,k)$ corresponds to the eigenvalues $E_{3,4}(\mathbf{k}) = -E_{2,1}(\mathbf{k})$ found from $\det[\mathbf{A}^{-1}(-k)]^T = 0$.

Using Eq. (D3) to write the fluctuation action as $\mathcal{S}_F = \int_0^\beta d\tau \int d^3\mathbf{r}\mathcal{L}_F(\mathbf{r},\tau)$ results in

$$\mathcal{S}_F = \beta V \sum_q \frac{|\Delta_q|^2}{\Gamma(q)} + \frac{\beta V}{2} \sum_{q_1,q_2,q_3} b_{1,2,3}\Delta_1\Delta_2^*\Delta_3\Delta_{1-2+3}^* + \frac{\beta V}{3} \sum_{q_1\cdots q_5} f_{1\cdots5}\Delta_1\Delta_2^*\Delta_3\Delta_4^*\Delta_5\Delta_{1-2+3-4+5}^*, \tag{D10}$$

where summation over $q \equiv (iq_n, \mathbf{q})$ indicates sums over both the bosonic Matsubara frequencies $q_n = 2\pi nT$ and momentum $\mathbf{q}$. Here, we used the shorthand notation $j \equiv q_j$ to represent the labels of Δ_{q_j} or $\Delta_{q_j}^*$.

The quadratic order appearing in Eq. (D10) arises from the terms $|\Delta(\mathbf{r},\tau)|^2/g$ and $(T/2V)\mathrm{Tr}(\mathbf{G}_0\mathbf{G}_F^{-1})^2/2$ in Eq. (D3), and is directly related to the pair propagator $\chi_{pair}(q) = V\Gamma^{-1}(q)$, with

$$\Gamma^{-1}(q) = \frac{1}{g} - \frac{T}{2V}\sum_k \frac{\mathrm{Tr}[\mathbf{A}(k)\mathbf{A}^{-1}(q-k)]}{\det[\mathbf{A}^{-1}(q-k)]}, \tag{D11}$$

where we use the identity $\boldsymbol{\sigma}_y\mathbf{A}\boldsymbol{\sigma}_y = \det(\mathbf{A})(\mathbf{A}^T)^{-1}$.

The fourth-order contribution arises from $\frac{1}{4}(\mathbf{G}_0\mathbf{G}_F^{-1})^4$ and leads to

$$b(q_1,q_2,q_3) = \frac{T}{2V}\sum_k \frac{\mathrm{Tr}[\mathbf{A}(k)\mathbf{A}^{-1}(q_1-k)\mathbf{A}(k-q_1+q_2)\mathbf{A}^{-1}(q_1-q_2+q_3-k)]}{\det[\mathbf{A}^{-1}(q_1-k)]\det[\mathbf{A}^{-1}(q_1-q_2+q_3-k)]}, \tag{D12}$$

while the sixth-order contribution emergences from $\frac{1}{6}(\mathbf{G}_0\mathbf{G}_F^{-1})^6$, giving

$$\begin{aligned} f(q_1,\ldots,q_5) = \frac{T}{2V}\sum_k & \det[\mathbf{A}(q_1-k)]\det[\mathbf{A}(q_1-q_2+q_3-k)]\det[\mathbf{A}(q_1-q_2+q_3-q_4+q_5-k)] \\ & \times\mathrm{Tr}[\mathbf{A}(k)\mathbf{A}^{-1}(q_1-k)\mathbf{A}(k-q_1+q_2)\mathbf{A}^{-1}(q_1-q_2+q_3-k) \\ & \times\mathbf{A}(k-q_1+q_2-q_3+q_4)\mathbf{A}^{-1}(q_1-q_2+q_3-q_4+q_5-k)]. \end{aligned} \tag{D13}$$

Evaluating the expressions given in Eqs. (D11) through (D13) requires us to perform summations over Matsubara frequencies of the type

$$T\sum_{i\omega_n} \frac{1}{i\omega_n \pm E(\mathbf{k})} = \begin{cases} n(\mathbf{k}) & \text{if "+"} \\ 1-n(\mathbf{k}) & \text{if "−"}, \end{cases} \tag{D14}$$

where $n(\mathbf{k}) = 1/[e^{\beta E(\mathbf{k})}+1]$ is the Fermi function. For the quadratic term, we obtain the result

$$\Gamma^{-1}(\mathbf{q}, iq_n) = -\frac{m}{4\pi a_s} + \frac{1}{2V}\sum_{\mathbf{k}}\left[\frac{1}{\varepsilon_{\mathbf{k}}} + \sum_{i,j=1}^{2}\alpha_{ij}(\mathbf{k},\mathbf{q})W_{ij}(\mathbf{k},\mathbf{q},iq_n)\right], \tag{D15}$$

where the functions in the last term are

$$W_{ij}(\mathbf{k},\mathbf{q},iq_n) = \frac{1-n_i(\mathbf{k})-n_j(\mathbf{k}+\mathbf{q})}{iq_n - E_i(\mathbf{k}) - E_j(\mathbf{k}+\mathbf{q})}, \tag{D16}$$

corresponding to the contribution of bubble diagrams to the pair susceptibility. The coherence factors are

$$\alpha_{11}(\mathbf{k},\mathbf{q}) = |u_{\mathbf{k}}u_{\mathbf{k}+\mathbf{q}} - v_{\mathbf{k}}v_{\mathbf{k}+\mathbf{q}}^*|^2, \tag{D17}$$

$$\alpha_{12}(\mathbf{k},\mathbf{q}) = |u_{\mathbf{k}}v_{\mathbf{k}+\mathbf{q}} + u_{\mathbf{k}+\mathbf{q}}v_{\mathbf{k}}|^2, \tag{D18}$$

with $\alpha_{11}(\mathbf{k},\mathbf{q}) = \alpha_{22}(\mathbf{k},\mathbf{q})$ and $\alpha_{12}(\mathbf{k},\mathbf{q}) = \alpha_{21}(\mathbf{k},\mathbf{q})$, where the quasiparticle amplitudes are

$$u_{\mathbf{k}} = \sqrt{\frac{1}{2}\left(1+\frac{h_z}{h_{\mathbf{k}}}\right)}, \tag{D19}$$

$$v_{\mathbf{k}} = e^{i\theta_{\mathbf{k}}}\sqrt{\frac{1}{2}\left(1-\frac{h_z}{h_{\mathbf{k}}}\right)}. \tag{D20}$$

The angle $\theta_{\mathbf{k}}$ is the phase associated with the spin-orbit field $h_{\perp}(\mathbf{k}) = |h_{\perp}(\mathbf{k})|e^{i\theta_{\mathbf{k}}}$, and we replaced the interaction parameter g by the s-wave scattering length a_s via Eq. (B7), recalling that $\varepsilon_{\mathbf{k}} = \mathbf{k}^2/2m$. The phase and modulus of $h_{\perp}(\mathbf{k})$ are

$$\theta_{\mathbf{k}} = \arctan\left(\frac{\eta k_y}{k_x}\right), \tag{D21}$$

$$|h_{\perp}(\mathbf{k})| = \frac{|\kappa|}{m}\sqrt{k_x^2+\eta k_y^2}, \tag{D22}$$

and the total effective field is

$$h_{\mathbf{k}} = \sqrt{h_z^2 + |h_\perp(\mathbf{k})|^2}. \tag{D23}$$

Since we are interested only in the long-wavelength and low-frequency regime, we perform an analytic continuation to real frequencies $iq_n = \omega + i\delta$ after calculating the Matsubara sums for all coefficients appearing in Eq. (D10) and perform a small momentum $\mathbf{q}$ and low-frequency ω expansion resulting in the Ginzburg-Landau action,

$$\begin{aligned}\mathcal{S}_F = \mathcal{S}_{GL} = \beta V \sum_q \left(a + \sum_\ell c_\ell \frac{q_\ell^2}{2m} - d_0\omega\right)|\Delta_q|^2 \\ + \frac{\beta V}{2} \sum_{q_1,q_2,q_3} b(q_1,q_2,q_3)\Delta_{q_1}\Delta^*_{q_2}\Delta_{q_3}\Delta^*_{q_1-q_2+q_3} \\ + \frac{\beta V}{3} \sum_{q_1\cdots q_5} f(q_1,q_2,q_3,q_4,q_5)\Delta_{q_1}\Delta^*_{q_2} \\ \times \Delta_{q_3}\Delta^*_{q_4}\Delta_{q_5}\Delta^*_{q_1-q_2+q_3-q_4+q_5}.\end{aligned} \tag{D24}$$

Here, the label ℓ appearing explicitly in the term $\sum_\ell c_\ell q_\ell^2/(2m)$ represents the spatial directions $\{x, y, z\}$, while the q_j's in the sums correspond to $(\mathbf{q}_j, \omega_j)$ and the summations $\sum_{q_j}$ represent integrals $\beta V \int d\omega_j \int d^3\mathbf{q}_j$, where j labels a fermion pair and can take values in the set $\{1, 2, 3, 4, 5\}$. In the expression above, we used the result

$$\Gamma^{-1}(\mathbf{q},\omega) = a + \sum_\ell c_\ell \frac{q_\ell^2}{2m} - d_0\omega + \cdots \tag{D25}$$

for the analytically continued expression of $\Gamma^{-1}(\mathbf{q}, iq_n)$ appearing in Eq. (D15). To write the coefficients above in a more compact notation, we define

$$X_i = X_i(\mathbf{k}) = \tanh[\beta E_i(\mathbf{k})/2], \tag{D26}$$

$$Y_i = Y_i(\mathbf{k}) = \mathrm{sech}^2[\beta E_i(\mathbf{k})/2]. \tag{D27}$$

The frequency- and momentum-independent coefficient is

$$\begin{aligned}a = -\frac{m}{4\pi a_s} + \frac{1}{V}\sum_{\mathbf{k}}\Bigg[\frac{1}{2\varepsilon_{\mathbf{k}}} - \left(\frac{X_1}{4E_1} + \frac{X_2}{4E_2}\right) \\ - \frac{h_z^2}{\xi_{\mathbf{k}} h_{\mathbf{k}}}\left(\frac{X_1}{4E_1} - \frac{X_2}{4E_2}\right)\Bigg],\end{aligned} \tag{D28}$$

where $E_1 = E_1(\mathbf{k})$ and $E_2 = E_2(\mathbf{k})$. The coefficient $d_0 = d_R + id_I$ multiplying the linear term in frequency has a real component given by

$$d_R = \frac{1}{2V}\mathcal{P}\sum_{\mathbf{k}}\sum_{i,j=1}^{2}\alpha_{ij}(\mathbf{k},\mathbf{0})\frac{1 - n_i(\mathbf{k}) - n_j(\mathbf{k})}{[E_i(\mathbf{k}) + E_j(\mathbf{k})]^2}. \tag{D29}$$

Using the explicit forms of the coherence factors $u_{\mathbf{k}}$ and $v_{\mathbf{k}}$ that define $\alpha_{ij}(\mathbf{k}, \mathbf{q} = \mathbf{0})$, the above expression can be rewritten as

$$\begin{aligned}d_R = \frac{1}{2V}\mathcal{P}\sum_{\mathbf{k}}\Bigg[\left(1 + \frac{h_z^2}{\xi_{\mathbf{k}}^2}\right)\left(\frac{X_1}{4E_1^2} + \frac{X_2}{4E_2^2}\right) \\ + \frac{2h_z^2}{\xi_{\mathbf{k}} h_{\mathbf{k}}}\left(\frac{X_1}{4E_1^2} - \frac{X_2}{4E_2^2}\right)\Bigg],\end{aligned} \tag{D30}$$

which defines the timescale for temporal oscillations of the order parameter. Here, the symbol $\mathcal{P}$ denotes the principal value, and the coefficient d_R is obtained from

$$\mathrm{Re}[\Gamma^{-1}(\mathbf{q} = \mathbf{0}, \omega + i\delta)] = -\frac{m}{4\pi a_s} + \frac{1}{2V}\sum_{\mathbf{k}}\left[\frac{1}{\varepsilon_{\mathbf{k}}} + \mathcal{P}\sum_{i,j=1}^{2}\alpha_{ij}(\mathbf{k},\mathbf{q}=\mathbf{0})\frac{1 - n_i(\mathbf{k}) - n_j(\mathbf{k})}{\omega - E_i(\mathbf{k}) - E_j(\mathbf{k})}\right]. \tag{D31}$$

The imaginary component of the coefficient d has the form

$$d_I = \frac{\pi}{2V}\sum_{\mathbf{k}}\sum_{i,j=1}^{2}\alpha_{ij}(\mathbf{k},\mathbf{0})[1 - n_i(\mathbf{k}) - n_j(\mathbf{k})]\delta'(E_i(\mathbf{k}) + E_j(\mathbf{k})), \tag{D32}$$

where the derivative of the δ function is $\delta'(\lambda) = \partial\delta(x + \lambda)/\partial x|_{x=0}$. Using again the expressions of the coherence factors $u_{\mathbf{k}}$ and $v_{\mathbf{k}}$ leads to

$$d_I = \frac{\pi}{2V}\sum_{\mathbf{k}}\left\{(X_1 + X_2)\delta'(2\xi_{\mathbf{k}}) + \frac{|h_\perp|^2}{h_{\mathbf{k}}^2}[X_1\delta'(2E_1) + X_2\delta'(2E_2) - (X_1 + X_2)\delta'(2\xi_{\mathbf{k}})]\right\}, \tag{D33}$$

which determines the lifetime of fermion pairs. This result originates from

$$\mathrm{Im}[\Gamma^{-1}(\mathbf{q} = \mathbf{0}, \omega + i\delta)] = -\frac{\pi}{2V}\sum_{\mathbf{k}}\sum_{i,j=1}^{2}\alpha_{ij}(\mathbf{k},\mathbf{q}=\mathbf{0})[1 - n_i(\mathbf{k}) - n_j(\mathbf{k})]\delta(\omega - E_i(\mathbf{k}) - E_j(\mathbf{k})), \tag{D34}$$

which immediately reveals that below the two-particle threshold $\omega_{tp}(\mathbf{q} = \mathbf{0}) = \min_{\{i,j,\mathbf{k}\}}[E_i(\mathbf{k}) + E_j(\mathbf{k})]$ at center-of-mass momentum $\mathbf{q} = \mathbf{0}$, the lifetime of the pairs is infinitely long due to the emergence of stable two-body bound states. Note that collisions between bound states are not yet included.

The expressions for the c_ℓ coefficients appearing in Eq. (D25) are quite long and complex. Since these coefficients are responsible for the mass renormalization and anisotropy within the Ginzburg-Landau theory, we outline below their derivation in detail. These coefficients can be obtained from

the last term in Eq. (D15), which we define as

$$F(\mathbf{q}) = \frac{1}{2V}\sum_{\mathbf{k}}\sum_{i,j=1}^{2}\alpha_{ij}(\mathbf{k},\mathbf{q})W_{ij}(\mathbf{k},\mathbf{q},iq_n=0). \tag{D35}$$

The relation between c_ℓ and the function $F(\mathbf{q})$ defined above is

$$c_\ell = m\left[\frac{\partial^2 F(\mathbf{q})}{\partial q_\ell^2}\right]_{\mathbf{q}=\mathbf{0}}. \tag{D36}$$

A more explicit form of c_ℓ is obtained by analyzing the symmetry properties of $F(\mathbf{q})$ under inversion and reflection symmetries. To make these properties clear, we rewrite the summand in Eq. (D35) by making use of the transformation $\mathbf{k}\to\mathbf{k}-\mathbf{q}/2$. This procedure leads to the symmetric form,

$$F(\mathbf{q}) = \frac{1}{2V}\sum_{\mathbf{k}}\sum_{i,j=1}^{2}\widetilde{\alpha}_{ij}(\mathbf{k}_-,\mathbf{k}_+)\widetilde{W}_{ij}[E_i(\mathbf{k}_-),E_j(\mathbf{k}_+)]. \tag{D37}$$

Here, $\mathbf{k}_+=\mathbf{k}+\mathbf{q}/2$ and $\mathbf{k}_-=\mathbf{k}-\mathbf{q}/2$ are new momentum labels, and

$$\widetilde{\alpha}_{11}(\mathbf{k}_-,\mathbf{k}_+) = |u_{\mathbf{k}_-}u_{\mathbf{k}_+} - v_{\mathbf{k}_-}v^*_{\mathbf{k}_+}|^2, \tag{D38}$$

$$\widetilde{\alpha}_{12}(\mathbf{k}_-,\mathbf{k}_+) = |u_{\mathbf{k}_-}v_{\mathbf{k}_+} - v_{\mathbf{k}_-}u_{\mathbf{k}_+}|^2 \tag{D39}$$

are coherence factors, with $\widetilde{\alpha}_{11}(\mathbf{k}_-,\mathbf{k}_+)=\widetilde{\alpha}_{22}(\mathbf{k}_-,\mathbf{k}_+)$ and $\widetilde{\alpha}_{12}(\mathbf{k}_-,\mathbf{k}_+)=\widetilde{\alpha}_{21}(\mathbf{k}_-,\mathbf{k}_+)$ The functions $u_{\mathbf{k}_\pm}$ and $v_{\mathbf{k}_\pm}$ are defined in Eqs. (D19) and (D20). It is now very easy to show that $\widetilde{\alpha}_{ij}(\mathbf{k}_-,\mathbf{k}_+)=\widetilde{\alpha}_{ij}(\mathbf{k}_+,\mathbf{k}_-)$, that is, $\widetilde{\alpha}_{ij}(\mathbf{k}_-,\mathbf{k}_+)$ is an even function of $\mathbf{q}$, since taking $\mathbf{q}\to-\mathbf{q}$ leads to $\mathbf{k}_-\to\mathbf{k}_+$ and $\mathbf{k}_+\to\mathbf{k}_-$, leaving $\widetilde{\alpha}_{ij}$ invariant. It is also clear, from its definition, that $\widetilde{\alpha}_{ij}$ is symmetric in the band indices $\{i,j\}$. Furthermore, the function

$$\widetilde{W}_{ij}[E_i(\mathbf{k}_-),E_j(\mathbf{k}_+)] = \frac{\mathcal{N}_{ij}}{\mathcal{D}_{ij}}, \tag{D40}$$

defined above, is the ratio between the numerator,

$$\mathcal{N}_{ij} = \tanh[\beta E_i(\mathbf{k}_-)/2] + \tanh[\beta E_j(\mathbf{k}_+)/2], \tag{D41}$$

representing the Fermi occupations, and the denominator,

$$\mathcal{D}_{ij} = 2[E_i(\mathbf{k}_-)+E_j(\mathbf{k}_+)], \tag{D42}$$

representing the sum of the quasiparticle excitation energies. To eliminate the Fermi distributions $n_i(\mathbf{k})$ in the numerator, we used the relation $1-2n_i(\mathbf{k})=\tanh[\beta E_i(\mathbf{k}_-)/2]$. Notice that $\widetilde{W}_{ij}[E_i(\mathbf{k}_-),E_j(\mathbf{k}_+)]$ is not generally symmetric under inversion $\mathbf{q}\to-\mathbf{q}$, that is, under the transformation $\mathbf{k}_-\to\mathbf{k}_+$ and $\mathbf{k}_+\to\mathbf{k}_-$. This means that $\widetilde{W}_{ij}[E_i(\mathbf{k}_-),E_j(\mathbf{k}_+)]\neq\widetilde{W}_{ij}[E_i(\mathbf{k}_+),E_j(\mathbf{k}_-)]$, unless when $i=j$, where it is trivially an even function of $\mathbf{q}$. However, $\widetilde{W}_{ij}[E_i(\mathbf{k}_-),E_j(\mathbf{k}_+)]$ is always symmetric under simultaneous momentum inversion ($\mathbf{q}\to-\mathbf{q}$) and band index exchange, that is,

$$\widetilde{W}_{ij}[E_i(\mathbf{k}_-),E_j(\mathbf{k}_+)] = \widetilde{W}_{ji}[E_j(\mathbf{k}_+),E_i(\mathbf{k}_-)], \tag{D43}$$

for any $\{i,j\}$. This property will be used later to write a final expression for c_ℓ. Next, we write

$$\left[\frac{\partial^2 F(\mathbf{q})}{\partial q_\ell^2}\right]_{\mathbf{q}=\mathbf{0}} = \frac{1}{2V}\sum_{\mathbf{k}}\sum_{i,j=1}^{2}\mathcal{F}_{ij}, \tag{D44}$$

where the function inside the summation is

$$\mathcal{F}_{ij} = \left[\frac{\partial^2\widetilde{\alpha}_{ij}}{\partial q_\ell^2}\widetilde{W}_{ij} + \alpha_{ij}\frac{\partial^2\widetilde{W}_{ij}}{\partial q_\ell^2}\right]_{\mathbf{q}=\mathbf{0}}. \tag{D45}$$

Notice the absence of terms containing the product of the first-order derivatives of $\widetilde{\alpha}_{ij}$ and $\widetilde{W}_{ij}$. These terms vanish due to parity since $\widetilde{\alpha}_{ij}$ is an even function of $\mathbf{q}$, leading to $[\partial\widetilde{\alpha}_{ij}/\partial q_\ell]_{\mathbf{q}=\mathbf{0}}=0$. The last expression can be further developed upon summation over the band indices, leading to

$$\left[\frac{\partial^2 F(\mathbf{q})}{\partial q_\ell^2}\right]_{\mathbf{q}=\mathbf{0}} = \mathcal{A}+\mathcal{B}. \tag{D46}$$

The first contribution is given by

$$\mathcal{A} = \frac{1}{2V}\sum_{\mathbf{k}}\left[\frac{\partial^2\widetilde{\alpha}_{11}}{\partial q_\ell^2}\widetilde{W}_{di} + \frac{\partial^2\widetilde{\alpha}_{12}}{\partial q_\ell^2}\widetilde{W}_{od}\right]_{\mathbf{q}=\mathbf{0}}, \tag{D47}$$

and contains the second derivatives of $\widetilde{\alpha}_{ij}$ and the symmetric terms

$$\widetilde{W}_{di} = (\widetilde{W}_{11}+\widetilde{W}_{22}), \tag{D48}$$

$$\widetilde{W}_{od} = (\widetilde{W}_{12}+\widetilde{W}_{21}). \tag{D49}$$

The second contribution is given by

$$\mathcal{B} = \frac{1}{2V}\sum_{\mathbf{k}}\left[\widetilde{\alpha}_{11}\frac{\partial^2\widetilde{W}_{di}}{\partial q_\ell^2} + \widetilde{\alpha}_{12}\frac{\partial^2\widetilde{W}_{od}}{\partial q_\ell^2}\right]_{\mathbf{q}=\mathbf{0}}. \tag{D50}$$

Next, we explicitly write $\widetilde{\alpha}_{ij}$, $\widetilde{W}_{ij}$ and their second derivatives with respect to q_ℓ at $\mathbf{q}=\mathbf{0}$. We start with

$$[\widetilde{W}_{ij}]_{\mathbf{q}=\mathbf{0}} = \frac{X_i+X_j}{2[E_i+E_j]}, \tag{D51}$$

and for the second derivative, we write

$$\left[\frac{\partial^2\widetilde{W}_{ij}}{\partial q_\ell^2}\right]_{\mathbf{q}=\mathbf{0}} = \left[\frac{1}{\mathcal{D}_{ij}}\frac{\partial^2\mathcal{N}_{ij}}{\partial q_\ell^2}\right]_{\mathbf{q}=\mathbf{0}} - \left[\frac{2}{\mathcal{D}_{ij}^2}\frac{\partial\mathcal{D}_{ij}}{\partial q_\ell}\frac{\partial\mathcal{N}_{ij}}{\partial q_\ell}\right]_{\mathbf{q}=\mathbf{0}} + \left[\frac{2\mathcal{N}_{ij}}{\mathcal{D}_{ij}^3}\left(\frac{\partial\mathcal{D}_{ij}}{\partial q_\ell}\right)^2\right]_{\mathbf{q}=\mathbf{0}} - \left[\frac{\mathcal{N}_{ij}}{\mathcal{D}_{ij}^2}\frac{\partial^2\mathcal{D}_{ij}}{\partial q_\ell^2}\right]_{\mathbf{q}=\mathbf{0}}.$$

Each one of the four terms in the above expression is evaluated at $\mathbf{q}=\mathbf{0}$ and can be written in terms of specific expressions that are given below. The numerator is

$$[\mathcal{N}_{ij}]_{\mathbf{q}=\mathbf{0}} = X_i+X_j, \tag{D52}$$

the first derivative of $\mathcal{N}_{ij}$ is

$$\left[\frac{\partial\mathcal{N}_{ij}}{\partial q_\ell}\right]_{\mathbf{q}=\mathbf{0}} = \frac{Y_j^2}{4T}\frac{\partial E_j}{\partial k_\ell} - \frac{Y_i^2}{4T}\frac{\partial E_i}{\partial k_\ell}, \tag{D53}$$

and the second derivative of $\mathcal{N}_{ij}$ is

$$\left[\frac{\partial^2\mathcal{N}_{ij}}{\partial q_\ell^2}\right]_{\mathbf{q}=\mathbf{0}} = -\frac{X_jY_j^2}{8T^2}\left(\frac{\partial E_j}{\partial k_\ell}\right)^2 + \frac{Y_i}{8T}\frac{\partial^2 E_i}{\partial k_\ell^2} - \frac{X_iY_i^2}{8T^2}\left(\frac{\partial E_i}{\partial k_\ell}\right)^2 + \frac{Y_i^2}{8T}\frac{\partial^2 E_i}{\partial k_\ell^2}. \tag{D54}$$

The denominator $\mathcal{D}_{ij}$ and its first derivative are

$$[\mathcal{D}_{ij}]_{\mathbf{q}=\mathbf{0}} = 2(E_i + E_j), \tag{D55}$$

$$\left[\frac{\partial \mathcal{D}_{ij}}{\partial q_\ell}\right]_{\mathbf{q}=\mathbf{0}} = \frac{\partial E_j}{\partial k_\ell} - \frac{\partial E_i}{\partial k_\ell}, \tag{D56}$$

while the second derivative of $\mathcal{D}_{ij}$ is

$$\left[\frac{\partial^2 \mathcal{D}_{ij}}{\partial q_\ell^2}\right]_{\mathbf{q}=\mathbf{0}} = \frac{1}{2}\left[\frac{\partial^2 E_i}{\partial k_\ell^2} + \frac{\partial^2 E_j}{\partial k_\ell^2}\right]. \tag{D57}$$

When the order parameter is zero, that is, $|\Delta_0| = 0$, the energies $E_1(\mathbf{k})$ and $E_2(\mathbf{k})$ become

$$E_1(\mathbf{k}) = ||\xi_\mathbf{k}| + h_\mathbf{k}|, \tag{D58}$$

$$E_2(\mathbf{k}) = ||\xi_\mathbf{k}| - h_\mathbf{k}|. \tag{D59}$$

The first derivatives of these energies are

$$\frac{\partial E_1(\mathbf{k})}{\partial k_\ell} = S_1(\mathbf{k})\frac{k_\ell}{m} + \frac{\partial h_\mathbf{k}}{\partial k_\ell}, \tag{D60}$$

$$\frac{\partial E_2(\mathbf{k})}{\partial k_\ell} = S_2(\mathbf{k})\frac{k_\ell}{m} - \frac{\partial h_\mathbf{k}}{\partial k_\ell}, \tag{D61}$$

with the functions $S_1(\mathbf{k}) = \mathrm{sgn}[|\xi_\mathbf{k}| + h_\mathbf{k}]\mathrm{sgn}[\xi_\mathbf{k}]$ and $S_2(\mathbf{k}) = \mathrm{sgn}[|\xi_\mathbf{k}| - h_\mathbf{k}]\mathrm{sgn}[\xi_\mathbf{k}]$. The derivative of the effective Zeeman field is

$$\frac{\partial h_\mathbf{k}}{\partial k_\ell} = \frac{1}{h_\mathbf{k}}\frac{\kappa^2}{m^2}(k_x\delta_{\ell x} + \eta k_y \delta_{\ell y}). \tag{D62}$$

The second derivatives of the energies are

$$\frac{\partial^2 E_1(\mathbf{k})}{\partial k_\ell^2} = \frac{S_1(\mathbf{k})}{m} + \frac{\partial^2 h_\mathbf{k}}{\partial k_\ell^2}, \tag{D63}$$

$$\frac{\partial^2 E_2(\mathbf{k})}{\partial k_\ell^2} = \frac{S_2(\mathbf{k})}{m} - \frac{\partial^2 h_\mathbf{k}}{\partial k_\ell^2}, \tag{D64}$$

where the second derivative of the effective field is

$$\frac{\partial^2 h_\mathbf{k}}{\partial k_\ell^2} = \frac{1}{h_\mathbf{k}}\frac{\kappa^2}{m^2}\left[(\delta_{\ell x} + \eta\delta_{\ell y}) - \frac{1}{h_\mathbf{k}^2}\frac{\kappa^2}{m^2}\left(k_x^2\delta_{\ell x} + \eta^2 k_y^2 \delta_{\ell y}\right)\right]. \tag{D65}$$

Since the diagonal elements $\widetilde{W}_{ii}$ are even functions of $\mathbf{q}$ and so are $\mathcal{N}_{ii}$ and $\mathcal{D}_{ii}$, their expressions are simpler than in the general case discussed above because the first-order derivatives of $\mathcal{N}_{ii}$ and $\mathcal{D}_{ii}$ vanish. The surviving terms involve only the second derivatives of $\mathcal{N}_{ii}$ and $\mathcal{D}_{ii}$, leading to the expression

$$\left[\frac{\partial^2 \widetilde{W}_{ii}}{\partial q_\ell^2}\right]_{\mathbf{q}=\mathbf{0}} = \left[\frac{1}{\mathcal{D}_{ii}}\frac{\partial^2 \mathcal{N}_{ii}}{\partial q_\ell^2}\right]_{\mathbf{q}=\mathbf{0}} - \left[\frac{\mathcal{N}_{ii}}{\mathcal{D}_{ii}^2}\frac{\partial^2 \mathcal{D}_{ii}}{\partial q_\ell^2}\right]_{\mathbf{q}=\mathbf{0}}. \tag{D66}$$

Here, the numerator and denominator functions are

$$[\mathcal{N}_{ii}]_{\mathbf{q}=\mathbf{0}} = 2X_i \quad \text{and} \quad [\mathcal{D}_{ii}]_{\mathbf{q}=\mathbf{0}} = 4E_i, \tag{D67}$$

while their second derivatives are

$$\left[\frac{\partial^2 \mathcal{N}_{ii}}{\partial q_\ell^2}\right]_{\mathbf{q}=\mathbf{0}} = -\frac{X_i Y_i^2}{4T^2}\left(\frac{\partial E_i}{\partial k_\ell}\right)^2 + \frac{Y_i^2}{4T}\frac{\partial^2 E_i}{\partial k_\ell^2}, \tag{D68}$$

$$\left[\frac{\partial^2 \mathcal{D}_{ii}}{\partial q_\ell^2}\right]_{\mathbf{q}=\mathbf{0}} = \frac{\partial^2 E_i}{\partial k_\ell^2}. \tag{D69}$$

The next step in obtaining the c_ℓ coefficients is to analyze the functions $\widetilde{\alpha}_{ij}$ and their second derivatives. We begin by writing $\widetilde{\alpha}_{11}$ at $\mathbf{q} = \mathbf{0}$,

$$[\widetilde{\alpha}_{11}]_{\mathbf{q}=\mathbf{0}} = \left|u_\mathbf{k}^2 - |v_\mathbf{k}|^2\right|^2 = \frac{h_z^2}{h_\mathbf{k}^2}. \tag{D70}$$

To investigate the second derivative of $\widetilde{\alpha}_{11}$, we write

$$\widetilde{\alpha}_{11} = \gamma_{11}\gamma_{11}^*, \tag{D71}$$

where the complex function is given by

$$\gamma_{11} = u_{\mathbf{k}_-}u_{\mathbf{k}_+} - v_{\mathbf{k}_-}v_{\mathbf{k}_+}. \tag{D72}$$

In this case, we write the first derivative of $\widetilde{\alpha}_{11}$ as

$$\frac{\partial \widetilde{\alpha}_{11}}{\partial q_\ell} = \frac{\partial \gamma_{11}}{\partial q_\ell}\gamma_{11}^* + \gamma_{11}\frac{\partial \gamma_{11}^*}{\partial q_\ell}, \tag{D73}$$

and the second derivative as

$$\frac{\partial^2 \widetilde{\alpha}_{11}}{\partial q_\ell^2} = \frac{\partial^2 \gamma_{11}}{\partial q_\ell^2}\gamma_{11}^* + 2\frac{\partial \gamma_{11}}{\partial q_\ell}\frac{\partial \gamma_{11}^*}{\partial q_\ell} + \gamma_{11}\frac{\partial^2 \gamma_{11}^*}{\partial q_\ell^2}. \tag{D74}$$

To explore the symmetry with respect to $\mathbf{q}$, we express γ_{11} in terms of its odd and even components via the relation $\gamma_{11} = \gamma_{11,e} + \gamma_{11,o}$, where the even component $\gamma_{11,e} = [\gamma_{11}(\mathbf{q}) + \gamma_{11}(-\mathbf{q})]/2$ is

$$\gamma_{11,e} = u_{\mathbf{k}_-}u_{\mathbf{k}_+} - |v_{\mathbf{k}_-}||v_{\mathbf{k}_+}|\cos(\theta_{\mathbf{k}_-} - \theta_{\mathbf{k}_+}), \tag{D75}$$

and the odd component $\gamma_{11,o} = [\gamma_{11}(\mathbf{q}) - \gamma_{11}(-\mathbf{q})]/2$ is

$$\gamma_{11,o} = i|v_{\mathbf{k}_+}||v_{\mathbf{k}_-}|\sin(\theta_{\mathbf{k}_+} - \theta_{\mathbf{k}_-}). \tag{D76}$$

Expressed via the even $\gamma_{11,e}$ and odd $\gamma_{11,o}$ components, the second derivative in Eq. (D74) is

$$\frac{\partial^2 \widetilde{\alpha}_{11}}{\partial q_\ell^2} = \frac{\partial^2 \gamma_{11,e}}{\partial q_\ell^2}\gamma_{11,e}^* + 2\frac{\partial \gamma_{11,o}}{\partial q_\ell}\frac{\partial \gamma_{11,o}^*}{\partial q_\ell} + \gamma_{11,e}\frac{\partial^2 \gamma_{11,e}^*}{\partial q_\ell^2}. \tag{D77}$$

Notice that the even component is purely real, that is, $\gamma_{11,e}^* = \gamma_{11,e}$, and that the odd component is purely imaginary, $\gamma_{11,o}^* = -\gamma_{11,o}$. Use of this property leads to

$$\frac{\partial^2 \widetilde{\alpha}_{11}}{\partial q_\ell^2} = 2\gamma_{11,e}\frac{\partial^2 \gamma_{11,e}}{\partial q_\ell^2} - 2\left(\frac{\partial \gamma_{11,o}}{\partial q_\ell}\right)^2. \tag{D78}$$

The contribution from the even term $\gamma_{11,e}$ is

$$[\gamma_{11,e}]_{\mathbf{q}=\mathbf{0}} = u_\mathbf{k}^2 - |v_\mathbf{k}|^2 = \frac{h_z}{h_\mathbf{k}}, \tag{D79}$$

and from its second derivative is

$$\left[\frac{\partial^2 \gamma_{11,e}}{\partial q_\ell^2}\right]_{\mathbf{q}=\mathbf{0}} = \frac{1}{2}\left(\frac{\partial |v_\mathbf{k}|}{\partial k_\ell}\right)^2 - \frac{1}{2}|v_\mathbf{k}|\frac{\partial^2 |v_\mathbf{k}|}{\partial k_\ell^2} + |v_\mathbf{k}|^2\left(\frac{\partial \theta_\mathbf{k}}{\partial k_\ell}\right)^2, \tag{D80}$$

while the contribution from the odd term $\gamma_{11,o}$ is

$$\left[\frac{\partial \gamma_{11,o}}{\partial q_\ell}\right]_{\mathbf{q}=\mathbf{0}} = i|v_\mathbf{k}|^2\frac{\partial \theta_\mathbf{k}}{\partial k_\ell}. \tag{D81}$$

Now, we turn our attention to $\widetilde{\alpha}_{12}$ and its second derivative. From Eq. (D39), we notice that γ_{12} is explicitly odd in $\mathbf{q}$ because $\gamma_{12}(\mathbf{q}) = -\gamma_{12}(-\mathbf{q})$, since the operation $\mathbf{q} \to -\mathbf{q}$ takes $\mathbf{k}_- \to \mathbf{k}_+$ and vice versa, leading to

$$[\widetilde{\alpha}_{12}]_{\mathbf{q}=\mathbf{0}} = 0. \tag{D82}$$

To calculate the second derivative of $\widetilde{\alpha}_{12}$, we write

$$\widetilde{\alpha}_{12} = \gamma_{12}\gamma_{12}^*, \tag{D83}$$

where the complex function

$$\gamma_{12} = u_{\mathbf{k}_-} v_{\mathbf{k}_+} - v_{\mathbf{k}_-} u_{\mathbf{k}_+}. \tag{D84}$$

We relate $\partial^2\widetilde{\alpha}_{12}/\partial q_\ell^2$ to γ_{12} and its first and second derivatives via

$$\frac{\partial^2\widetilde{\alpha}_{12}}{\partial q_\ell^2} = \frac{\partial^2\gamma_{12}}{\partial q_\ell^2}\gamma_{12}^* + 2\frac{\partial\gamma_{12}}{\partial q_\ell}\frac{\partial\gamma_{12}^*}{\partial q_\ell} + \gamma_{12}\frac{\partial^2\gamma_{12}^*}{\partial q_\ell^2}. \tag{D85}$$

Given that $[\gamma_{12}]_{\mathbf{q}=\mathbf{0}} = 0$ and $[\gamma_{12}^*]_{\mathbf{q}=\mathbf{0}} = 0$, the expression above simplifies to

$$\left[\frac{\partial^2\widetilde{\alpha}_{12}}{\partial q_\ell^2}\right]_{\mathbf{q}=\mathbf{0}} = 2\left[\frac{\partial\gamma_{12}}{\partial q_\ell}\frac{\partial\gamma_{12}^*}{\partial q_\ell}\right]_{\mathbf{q}=\mathbf{0}} = [\Lambda_\ell(\mathbf{q})]^2, \tag{D86}$$

where we used the expressions

$$\left[\frac{\partial\gamma_{12}}{\partial q_\ell}\right]_{\mathbf{q}=\mathbf{0}} = e^{i\theta_{\mathbf{k}}}\Lambda_\ell(\mathbf{k}) \tag{D87}$$

for the derivatives of γ_{12} at $\mathbf{q} = \mathbf{0}$ with the function

$$\Lambda_\ell(\mathbf{k}) = u_{\mathbf{k}}\frac{\partial|v_{\mathbf{k}}|}{\partial k_\ell} - |v_{\mathbf{k}}|\frac{\partial u_{\mathbf{k}}}{\partial k_\ell} + u_{\mathbf{k}}|v_{\mathbf{k}}|\frac{\partial\theta_{\mathbf{k}}}{\partial k_\ell}. \tag{D88}$$

The last information needed is the derivatives of $u_{\mathbf{k}}$, $|v_{\mathbf{k}}|$, and $\theta_{\mathbf{k}}$, which are given by

$$\frac{\partial u_{\mathbf{k}}}{\partial k_\ell} = -\frac{1}{2}\frac{h_z}{h_{\mathbf{k}}^3}\frac{\kappa^2}{m^2}\frac{(k_x\delta_{\ell x} + \eta k_y\delta_{\ell y})}{(1 + h_z/h_{\mathbf{k}})^{1/2}}, \tag{D89}$$

$$\frac{\partial|v_{\mathbf{k}}|}{\partial k_\ell} = \frac{1}{2}\frac{h_z}{h_{\mathbf{k}}^3}\frac{\kappa^2}{m^2}\frac{(k_x\delta_{\ell x} + \eta k_y\delta_{\ell y})}{(1 - h_z/h_{\mathbf{k}})^{1/2}}, \tag{D90}$$

$$\frac{\partial\theta_{\mathbf{k}}}{\partial k_\ell} = \eta\frac{(k_x\delta_{\ell y} - k_y\delta_{\ell x})}{k_x^2 + \eta^2 k_y^2}. \tag{D91}$$

The long steps discussed above complete the derivation of all the functions needed to compute the c_ℓ coefficients for an arbitrary spin-orbit coupling, expressed as a general linear combination of Rashba and Dresselhaus terms.

As announced earlier, the calculation of c_ℓ, defined in Eq. (D36), is indeed very long and requires the use of all the expressions given from Eq. (D37) to Eq. (D91). Despite this complexity, that are a few important comments about the symmetries of the c_ℓ coefficients that are worth mentioning. Given that c_ℓ determines the mass anisotropies in the Ginzburg-Landau (GL) theory, we discuss next the anisotropies of c_ℓ as a function of the spin-orbit-coupling parameters κ and η. First, in the limit of zero spin-orbit coupling, where κ and η are equal to zero, all the c_ℓ coefficients are identical, reflecting the isotropy of the system, that is, $c_x = c_y = c_z$, and reduce to previously known results [51]. In this case, the GL effective masses $m_\ell = md_R/c_\ell$ are isotropic: $m_x = m_y = m_z$. Second, in the limit of $\kappa \neq 0$ and $\eta = \pm 1$, the spin-orbit coupling has the same strength along the x and y directions, and thus for the Rashba ($\eta = 1$) or Dresselhaus ($\eta = -1$) cases, the coefficients obey the relation $c_x = c_y \neq c_z$. This leads to effective masses $m_x = m_y \neq m_z$. Third, in the limit $\kappa \neq 0$, but $\eta = 0$, corresponding to the ERD case, the coefficients have the symmetry $c_x \neq c_y = c_z$. Now the effective masses obey the relation $m_x \neq m_y = m_z$. Finally, in the case where $\kappa \neq 0$, and $0 \neq |\eta| < 1$, all the c_ℓ coefficients are different, that is, $c_x \neq c_y \neq c_z$. Therefore, the effective masses are also different in all three directions: $m_x \neq m_y \neq m_z$.

Following an analogous procedure, we analyze the coefficients $b(q_1, q_2, q_3)$, and $e(q_1, q_2, q_3, q_4, q_5)$ with all $q_i = (0, 0)$, and define

$$Z_{ij} = X_i + \beta E_i Y_j/2. \tag{D92}$$

Using the notation $b(0, 0, 0) = b(0)$, we obtain

$$b(0) = \frac{1}{8V}\sum_{\mathbf{k}}\left[\left(1 + \frac{h_z^4}{\xi_{\mathbf{k}}^2 h_{\mathbf{k}}^2}\right)\left(\frac{Z_{11}}{E_1^3} + \frac{Z_{22}}{E_2^3}\right) + \frac{2h_z^2}{\xi_{\mathbf{k}} h_{\mathbf{k}}}\left(\frac{Z_{11}}{E_1^3} - \frac{Z_{22}}{E_2^3}\right) + \frac{h_z^4}{\xi_{\mathbf{k}}^3 h_{\mathbf{k}}^3}\left(\frac{X_1}{E_1} - \frac{X_2}{E_2}\right)\right], \tag{D93}$$

which is a measure of the local interaction between two pairing fields. Using the notation $f(0, 0, 0, 0, 0) = f(0)$, we obtain

$$\begin{aligned} f(0) = \frac{3}{32V}\sum_{\mathbf{k}}\Bigg[&-\left(1 + \frac{3h_z^4}{\xi_{\mathbf{k}}^2 h_{\mathbf{k}}^2}\right)\left(\frac{Z_{11}}{E_1^5} + \frac{Z_{22}}{E_2^5}\right) - \frac{h_z^2}{\xi_{\mathbf{k}} h_{\mathbf{k}}}\left(3 + \frac{h_z^4}{\xi_{\mathbf{k}}^2 h_{\mathbf{k}}^2}\right)\left(\frac{Z_{11}}{E_1^5} - \frac{Z_{22}}{E_2^5}\right) - \frac{h_z^6}{\xi_{\mathbf{k}}^4 h_{\mathbf{k}}^4}\left(\frac{Z_{11}}{E_1^3} + \frac{Z_{22}}{E_2^3}\right) \\ &- \frac{h_z^4}{\xi_{\mathbf{k}}^3 h_{\mathbf{k}}^3}\left(\frac{Z_{11}}{E_1^3} - \frac{Z_{22}}{E_2^3}\right) + \frac{\beta^2}{6}\left(\frac{X_1 Y_1}{E_1^3} + \frac{X_2 Y_2}{E_2^3}\right) + \frac{\beta^2 h_z^2}{6\xi_{\mathbf{k}} h_{\mathbf{k}}}\left(\frac{X_1 Y_1}{E_1^3} - \frac{X_2 Y_2}{E_2^3}\right) - \frac{h_z^6}{\xi_{\mathbf{k}}^5 h_{\mathbf{k}}^5}\left(\frac{X_1}{E_1} - \frac{X_2}{E_2}\right)\Bigg], \end{aligned} \tag{D94}$$

which is a measure of the local interaction between three pairing fields. It is important to mention that in the absence of spin-orbit and Zeeman fields, the Ginzburg-Landau coefficients obtained above reduce to those reported in the literature [51].

As we proceed to explicitly write the Ginzburg-Landau action and Lagrangian density, we emphasize that in contrast to the standard crossover that one observes in the absence of an external Zeeman field [51], for fixed $h_z \neq 0$ it is possible for the system to undergo a first-order phase transition with increasing $1/k_F a_s$. The same applies for fixed $1/k_F a_s$ with increasing h_z. Thus, while an expansion of $\mathcal{S}_F$ to quartic order is sufficient when no Zeeman fields are present, when Zeeman fields are turned on, the fourth-order coefficient $b(0) = b$ may become negative. Such a situation requires the analysis of the sixth-order coefficient $f(0) = f$ to describe this first-order transition correctly and to stabilize the theory since $f > 0$.

The Ginzburg-Landau action in Euclidean space can be written as $\mathcal{S}_{GL} = \int dt \int d^3\mathbf{r}\mathcal{L}_{GL}(r)$, where $r \equiv (\mathbf{r}, t)$. Here,

the Lagrangian density is

$$\mathcal{L}_{GL}(r) = a|\Delta(r)|^2 + \frac{b}{2}|\Delta(r)|^4 + \frac{f}{3}|\Delta(r)|^6 + \sum_\ell c_\ell \frac{|\nabla_\ell \Delta(r)|^2}{2m} - id_0\Delta^*(r)\frac{\partial\Delta(r)}{\partial t}, \quad \text{(D95)}$$

where $\ell = \{x, y, z\}$, $b = b(0)$, and $f = f(0)$. A variation of $\mathcal{S}_{GL}$ with respect to $\Delta^*(r)$ via $\delta\mathcal{S}_{GL}/\delta\Delta^*(r) = 0$ yields the time-dependent Ginzburg-Landau (TDGL) equation,

$$\left(-id_0\frac{\partial}{\partial t} - \sum_\ell c_\ell \frac{\nabla_\ell^2}{2m} + b|\Delta|^2 + f|\Delta|^4 + a\right)\Delta(r) = 0, \quad \text{(D96)}$$

with cubic and quintic terms, where $\Delta = \Delta(r)$ are dependent on space and time. This equation describes the spatiotemporal behavior of the order parameter $\Delta(\mathbf{r}, t)$ in the long-wavelength and long-time regime.

In the static homogeneous case with $b > 0$, Eq. (D96) reduces to either the trivial (normal-state) solution $\Delta = 0$ when $a > 0$ or to the nontrivial (superfluid state) $|\Delta| = \sqrt{|a|/b}$, when $a < 0$. The coefficient d provides the timescale of the TDGL equation, and thereby determines the lifetime associated with the pairing field $\Delta(r)$. This can be seen directly by again considering the homogeneous case to linear order in $\Delta(r)$, in which case the TDGL equation has the solution $\Delta(t) \approx \Delta(0)e^{iat/d_0}$. This last expression can be rewritten more explicitly as $\Delta(t) \approx \Delta(0)e^{-i\omega_0 t}e^{-t/\tau_0}$, where $\omega_0 = |a|d_R/|d_0|^2$ is the oscillation frequency of the pairing field, and $\tau_0 = |d_0|^2/(|a|d_I)$ is the lifetime of the pairs, where both d_R and d_I are positive definite, that is, $d_R > 0$ and $d_I > 0$.

In the BEC regime, where stable two-body bound states exist, the imaginary part of d_0 vanishes ($d_I = 0$), and the lifetime time of the pairs is infinitely long. In this case, $d_0 = d_R$ and we can define the effective bosonic wave function $\Psi = \sqrt{d_R}\Delta$ to recast Eq. (D96) in the form of the Gross-Pitaevskii equation,

$$\left(-i\frac{\partial}{\partial t} - \sum_\ell \frac{\nabla_\ell^2}{2M_\ell} + U_2|\Psi|^2 + U_3|\Psi|^4 - \mu_B\right)\Psi(r) = 0, \quad \text{(D97)}$$

with cubic and quintic nonlinearities, where $\Psi = \Psi(r)$, to describe a dilute Bose gas. Here, $\mu_B = -a/d_R$ is the bosonic chemical potential, $M_\ell = m(d_R/c_\ell)$ are the anisotropic masses of the bosons, and $U_2 = b/d_R^2$ and $U_3 = f/d_R^3$ represent contact interactions of two and three bosons, respectively. In the Bose regime, the lifetime τ of the composite boson is $\tau \propto 1/d_I \to \infty$ and the interactions U_2 and U_3 are always repulsive, thus leading to a system consisting of a dilute gas of stable bosons. In this regime, the chemical potential of the bosons is $\mu_B \approx 2\mu + E_b < 0$, where E_b is the two-body bound state energy in the presence of spin-orbit coupling and Zeeman fields obtained from the condition $\Gamma^{-1}(\mathbf{q}, E - 2\mu) = 0$ discussed in the main text. Notice that when $\mu_B \to 0^-$, in the absence of boson-boson interactions, the bosons condense.

[1] Y.-J. Lin, R. L. Compton, K. Jiminéz-García, J. V. Porto, and I. B. Spielman, Synthetic magnetic fields for ultracold neutral atoms, Nature (London) **462**, 628 (2009).

[2] Y-J. Lin, R. L. Compton, A. R. Perry, W. D. Phillips, J. V. Porto, and I. B. Spielman, Bose-Einstein Condensate in a Uniform Light-Induced Vector Potential, Phys. Rev. Lett. **102**, 130401 (2009).

[3] C. J. Kennedy, W. C. Burton, W. C. Chung, and W. Ketterle, Observation of Bose-Einstein condensation in a strong synthetic magnetic field, Nat. Phys. **11**, 859 (2015).

[4] Y.-J. Lin, K. Jiménez-García, and I. B. Spielman, Spin-orbit-coupled Bose-Einstein condensates, Nature (London) **471**, 83 (2011).

[5] L. W. Cheuk, A. T. Sommer, Z. Hadzibabic, T. Yefsah, W. S. Bakr, and M. W. Zwierlein, Spin-Injection Spectroscopy of a Spin-Orbit Coupled Fermi Gas, Phys. Rev. Lett. **109**, 095302 (2012).

[6] P. Wang, Z.-Q. Yu, Z. Fu, J. Miao, L. Huang, S. Chai, H. Zhai, and J. Zhang, Spin-Orbit Coupled Degenerate Fermi Gases, Phys. Rev. Lett. **109**, 095301 (2012).

[7] R. A. Williams, M. C. Beeler, L. J. LeBlanc, K. Jiménez-García and I. B. Spielman, Raman-Induced Interactions in a Single-Component Fermi Gas Near an s-Wave Feshbach Resonance, Phys. Rev. Lett. **111**, 095301 (2013).

[8] V. Galitski and I. B. Spielman, Spin-orbit coupling in quantum gases, Nature (London) **494**, 49 (2013).

[9] Z. Fu, L. Huang, Z. Meng, P. Wang, L. Zhang, S. Zhang, H. Zhai, P. Zhang, and J. Zhang, Production of Feshbach molecules induced by spin-orbit coupling in Fermi gases, Nat. Phys. **10**, 110 (2014).

[10] M. Mancini, G. Pagano, G. Cappellini, L. Livi, M. Rider, J. Catani, C. Sias, P. Zoller, M. Inguscio, M. Dalmonte, and L. Fallani, Observation of chiral edge states with neutral fermions in synthetic Hall ribbons, Science **349**, 1510 (2015).

[11] L. Huang, Z. Meng, P. Wang, P. Peng, S.-L. Zhang, L. Chen, D. Li, Q. Zhou, and J. Zhang, Experimental realization of two-dimensional synthetic spin-orbit coupling in ultracold Fermi gases, Nat. Phys. **12**, 540 (2016).

[12] Z. Wu, L. Zhang, W. Sun, X.-T. Xu, B.-Z. Wang, S.-C. Ji, Y. Deng, S. Chen, X.-J. Liu, and J.-W. Pan, Realization of two-dimensional spin-orbit coupling for Bose-Einstein condensates, Science **354**, 83 (2016).

[13] J. I. Cirac and P. Zoller, Goals and opportunities in quantum simulation, Nat. Phys. **8**, 264 (2012).

[14] U.-J. Wiese, Ultracold quantum gases and lattice systems: Quantum simulation of lattice gauge theories, Ann. Phys. **525**, 777 (2013).

[15] E. Zohar, J. I. Cirac, and B. Reznik, Quantum simulations of lattice gauge theories using ultracold atoms in optical lattices, Rep. Prog. Phys. **79**, 014401 (2016).

[16] M. Dalmonte and S. Montangero, Lattice gauge theory simulations in the quantum information era, Contemp. Phys. **57**, 388 (2016).

[17] M. Gong, S. Tewari, and C. Zhang, BCS-BEC Crossover and Topological Phase Transition in 3D Spin-Orbit Coupled Degenerate Fermi Gases, Phys. Rev. Lett. **107**, 195303 (2011).

[18] Z.-Q. Yu and H. Zhai, Spin-Orbit Coupled Fermi Gases across a Feshbach Resonance, Phys. Rev. Lett. **107**, 195305 (2011).

[19] H. Hu, L. Jiang, X.-J. Liu, and H. Pu, Probing Anisotropic Superfluidity in Atomic Fermi Gases with Rashba Spin-Orbit Coupling, Phys. Rev. Lett. **107**, 195304 (2011).

[20] L. Han and C. A. R. Sá de Melo, Evolution from BCS to BEC superfluidity in the presence of spin-orbit coupling, Phys. Rev. A **85**, 011606(R) (2012).

[21] K. Seo, L. Han, and C. A. R. Sá de Melo, Emergence of Majorana and Dirac Particles in Ultracold Fermions via Tunable Interactions, Spin-Orbit Effects, and Zeeman Fields, Phys. Rev. Lett. **109**, 105303 (2012).

[22] K. Seo, L. Han, and C. A. R. Sá de Melo, Topological phase transitions in ultracold Fermi superfluids: The evolution from Bardeen-Cooper-Schrieffer to Bose-Einstein-condensate superfluids under artificial spin-orbit fields, Phys. Rev. A **85**, 033601 (2012).

[23] D. M. Kurkcuoglu and C. A. R. Sá de Melo, Formation of Feshbach molecules in the presence of artificial spin-orbit coupling and Zeeman fields, Phys. Rev. A **93**, 023611 (2016).

[24] N. Goldman, I. Satija, P. Nikolic, A. Bermudez, M. A. Martin-Delgado, M. Lewenstein, and I. B. Spielman, Realistic Time-Reversal Invariant Topological Insulators with Neutral Atoms, Phys. Rev. Lett. **105**, 255302 (2010).

[25] I. B. Spielman (private communication).

[26] Gediminas Juzeliūnas, J. Ruseckas, and J. Dalibard, Generalized Rashba-Dresselhaus spin-orbit coupling for cold atoms, Phys. Rev. A **81**, 053403 (2010).

[27] D. L. Campbell, G. Juzeliūnas, and I. Spielman, Realistic Rashba and Dresselhaus spin-orbit coupling for neutral atoms, Phys. Rev. A **84**, 025602 (2011).

[28] G. Dresselhaus, Spin-orbit coupling effects in zinc blende structures, Phys. Rev. **100**, 580 (1955).

[29] E. I. Rashba, Properties of semiconductors with an extremum loop: I. Cyclotron and combinational resonance in a magnetic field perpendicular to the plane of the loop, Sov. Phys. Solid State **2**, 1224 (1960).

[30] C. A. R. Sá de Melo, When fermions become bosons: Pairing in ultracold gases, Phys. Today **61**, 45 (2008).

[31] T. Ozawa and G. Baym, Population imbalance and pairing in the BCS-BEC crossover of three-component ultracold fermions, Phys. Rev. A **82**, 063615 (2010).

[32] P. D. Powell, From quarks to cold atoms: The phases of strongly-interacting systems, Ph.D. thesis, University of Illinois at Urbana-Champaign, 2013.

[33] D. M. Kurkcuoglu and C. A. R. Sá de Melo, Color superfluidity of neutral ultracold fermions in the presence of color-flip and color-orbit fields, Phys. Rev. A **97**, 023632 (2018).

[34] D. Yamamoto, I. B. Spielman, and C. A. R. Sá de Melo, Quantum phases of two-component bosons with spin-orbit coupling in optical lattices, Phys. Rev. A **96**, 061603(R) (2017).

[35] S. L. Bromley, S. Kolkowitz, T. Bothwell, D. Kedar, A. Safavi-Naini, M. L. Wall, C. Salomon, A. M. Rey, and J. Ye, Dynamics of interacting fermions under spin-orbit coupling in an optical lattice clock, Nat. Phys. **14**, 399 (2018).

[36] Yu. Yi-Xiang, F. Sun, and J. Ye, Class of topological phase transitions of Rashba spin-orbit coupled fermions on a square lattice, Phys. Rev. B **98**, 174506 (2018).

[37] M. Mamaev, R. Blatt, J. Ye, and A. M. Rey, Cluster State Generation with Spin-Orbit Coupled Fermionic Atoms in Optical Lattices, Phys. Rev. Lett. **122**, 160402 (2019).

[38] B. Gong, S. Li, X.-H. Zhang, B. Liu, and W. Yi, Bloch bound state of spin-orbit-coupled fermions in an optical lattice, Phys. Rev. A **99**, 012703 (2019).

[39] M. H. Yau and C. A. R. Sá de Melo, Chern-number spectrum of ultracold fermions in optical lattices tuned independently via artificial magnetic, Zeeman, Spin-orbit fields, Phys. Rev. A **99**, 043625 (2019).

[40] W. Jia, Z.-H. Huang, X. Wei, Q. Zhao, and X.-J. Liu, Topological superfluids for spin-orbit coupled ultracold Fermi gases, Phys. Rev. B **99**, 094520 (2019).

[41] M. Kheirkhah, Z. Yan, Y. Nagai, and F. Marsiglio, First- and Second-Order Topological Superconductivity and Temperature-Driven Topological Phase Transitions in the Extended Hubbard Model with Spin-Orbit Coupling, Phys. Rev. Lett. **125**, 017001 (2020).

[42] U. Gebert, B. Irsigler, and W. Hofstetter, Local Chern marker of smoothly confined Hofstadter fermions, Phys. Rev. A **101**, 063606 (2020).

[43] I. Titvinidze, J. Legendre, M. Grothus, B. Irsigler, K. Le Hur, and W. Hofstetter, Spin-orbit coupling in the kagome lattice with flux and time-reversal symmetry, Phys. Rev. B **103**, 195105 (2021).

[44] R. A. Williams, L. J. LeBlanc, K. Jiménez-García, M. C. Beeler, A. R. Perry, W. D. Phillips, and I. B. Spielman, Synthetic partial waves in ultracold atomic collisions, Science **335**, 314 (2012).

[45] Z. Meng, L. Huang, P. Peng, D. Li, L. Chen, Y. Xu, C. Zhang, P. Wang, and J. Zhang Experimental Observation of a Topological Band Gap Opening in Ultracold Fermi Gases with Two-Dimensional Spin-Orbit Coupling, Phys. Rev. Lett. **117**, 235304 (2016).

[46] A. Valdés-Curiel, D. Trypogeorgos, Q.-Y. Liang, R. P. Anderson, and I. B. Spielman, Topological features without a lattice in Rashba spin-orbit coupled atoms, Nat. Commun. **12**, 593 (2021).

[47] R. M. Kroeze, Y. Guo, and B. L. Lev, Dynamical Spin-Orbit Coupling of a Quantum Gas, Phys. Rev. Lett. **123**, 160404 (2019).

[48] Z.-Y. Wang, X.-C. Cheng, B.-Z. Wang, J.-Y. Zhang, Y.-H. Lu, C.-R. Yi, S. Niu, Y. Deng, X.-J. Liu, S. Chen, and J.-W. Pan, Realization of an ideal Weyl semimetal band in a quantum gas with 3D spin-orbit coupling, Science **372**, 271 (2021).

[49] A. J. Leggett, in *Modern Trends in the Theory of Condensed Matter*, edited by A. Pekalski and R. Przystawa (Springer-Verlag, Berlin, 1980), pp. 13–27.

[50] J. R. Engelbrecht, M. Randeria, and C. A. R. Sá de Melo, BCS to Bose crossover: Broken-symmetry state, Phys. Rev. B **55**, 15153 (1997).

[51] C. A. R. Sá de Melo, M. Randeria, and J. Engelbrecht, Crossover from BCS to Bose Superconductivity: Transition Temperature and Time-Dependent Ginzburg-Landau Theory, Phys. Rev. Lett. **71**, 3202 (1993).

[52] P. D. Powell, G. Baym, and C. A. R. Sá de Melo, Superfluid transition temperature of spin-orbit and Rabi coupled fermions with tunable interactions, arXiv:1709.07042v1.

[53] S. Gopalakrishnan, A. Lamacraft, and P. M. Goldbart, Universal phase structure of dilute Bose gases with Rashba spin-orbit coupling, Phys. Rev. A **84**, 061604(R) (2011).

[54] T. Ozawa, Topics in multi-component ultracold gases and gauge fields, Ph.D. thesis, University of Illinois at Urbana-Champaign, 2012.

[55] P. Noziöres and S. Schmitt-Rink, Bose condensation in an attractive fermion gas: From weak to strong coupling superconductivity, J. Low Temp. Phys. **59**, 195 (1985).

[56] Z. Yu and G. Baym, Spin correlation functions in ultracold paired atomic-fermion systems: Sum rules, self-consistent approximations, and mean fields, Phys. Rev. A **73**, 063601 (2006).

[57] Z. Yu, G. Baym, and C. J. Pethick, Calculating energy shifts in terms of phase shifts, J. Phys. B: At. Mol. Opt. Phys. **44**, 195207 (2011).

[58] P. Fulde and R. A. Ferrell, Superconductivity in a strong spin-exchange field, Phys. Rev. **135**, A550 (1964).

[59] A. I. Larkin and Y. N. Ovchinnikov, Nonuniform state of superconductors, Sov. Phys. JETP **20**, 762 (1965).

[60] A. M. Clogston, Upper Limit for the Critical Field in Hard Superconductors, Phys. Rev. Lett. **9**, 266 (1962).

[61] G. Sarma, On the influence of a uniform exchange field acting on the spins of the conduction electrons in a superconductor, J. Phys. Chem. Solids **24**, 1029 (1963).

[62] G. Baym, J.-P. Blaizot, M. Holzmann, F. Laloë, and D. Vautherin, The Transition Temperature of the Dilute Interacting Bose Gas, Phys. Rev. Lett. **83**, 1703 (1999).

[63] M. Iskin and C. A. R. Sá de Melo, Fermi-Fermi mixtures in the strong-attraction limit, Phys. Rev. A **77**, 013625 (2008).

[64] D. S. Petrov, C. Salomon, and G. V. Shlyapnikov, Diatomic molecules in ultracold Fermi gases: Novel composite bosons, J. Phys. B: At. Mol. Opt. Phys. **38**, S645 (2005).

[65] J. P. Vyasanakere, S. Zhang, and V. B. Shenoy, BCS-BEC crossover induced by a synthetic non-Abelian gauge field, Phys. Rev. B **84**, 014512 (2011).

[66] X.-J. Feng and L. Yin, Phase diagram of a spin-orbit coupled dipolar Fermi gas at $T = 0$ K, Chin. Phys. Lett. **37**, 020301 (2020).

[67] L. Dell'Anna, G. Mazzarella, and L. Salasnich, Condensate fraction of a resonant Fermi gas with spin-orbit coupling in three and two dimensions, Phys. Rev. A **84**, 033633 (2011).

[68] L. Dell'Anna, G. Mazzarella, and L. Salasnich, Tuning Rashba and Dresselhaus spin-orbit couplings: Effects on singlet and triplet condensation with Fermi atoms, Phys. Rev. A **86**, 053632 (2012).

[69] S. Tewari, T. D. Stanescu, J. D. Sau, and S. Das Sarma, Topologically non-trivial superconductivity in spin-orbit-coupled systems: Bulk phases and quantum phase transitions, New J. Phys. **13**, 065004 (2011).

[70] L. Han and C. A. R. Sá de Melo, Ultra-cold fermions in the flatland: Evolution from BCS to Bose superfluidity in two-dimensions with spin-orbit and Zeeman fields, arXiv:1206.4984.

[71] J. P. A. Devreese, J. Tempere, and C. A. R. Sá de Melo, Effects of Spin-Orbit Coupling on the Berezinskii-Kosterlitz-Thouless Transition and the Vortex-Antivortex Structure in Two-Dimensional Fermi Gases, Phys. Rev. Lett. **113**, 165304 (2014).

[72] J. P. A. Devreese, J. Tempere, and C. A. R. Sá de Melo, Quantum phase transitions and Berezinskii-Kosterlitz-Thouless temperature in a two-dimensional spin-orbit-coupled Fermi gas, Phys. Rev. A **92**, 043618 (2015)

[73] J. P. Vyasanakere and V. B. Shenoy, Fluctuation theory of Rashba Fermi gases: Gaussian and beyond, Phys. Rev. B **92**, 121111(R) (2015).

[74] T. Yamaguchi, D. Inotani, and Y. Ohashi, Rashbon bound states associated with a spherical spin-orbit coupling in an ultracold Fermi gas with an s-wave interaction, J. Low Temp. Phys. **183**, 161 (2016).

[75] B. M. Anderson, C.-T. Wu, R. Boyack, and K. Levin, Topological effects on transition temperatures and response functions in three-dimensional Fermi superfluids, Phys. Rev. B **92**, 134523 (2015).

[76] L. Dell'Anna and S. Grava, Critical temperature in the BCS-BEC crossover with spin-orbit coupling, Condens. Matter **6**, 16 (2021).